International Journal of Science and Research (IJSR)
ISSN: 2319-7064
SJIF (2022): 7.94

Effect of Oil in Place on Sandstone Reservoir Quality of Dibeilla Prospect, Termit Basin, Niger: Insight from Pre-Stack Seismic Inversion and Diagenesis

Hamma Ada Moussa[1], Abdou Dodo Bohari[1], Hassan Ibrahim Maharou[1], Abdourahamane Ibrahim Ari Maïna[2], Moussa Harouna[1]

[1] Université Abdou Moumouni, Faculté des Sciences et Techniques, Département de Géologie, B. P. 10662, Niamey, Niger
[2]Pan African University of Life and Earth Science Institute, Ibadan, Nigeria
Corresponding-author: *hammamoussa [at]gmail.com*

Abstract: ***Paleogene Sokor1 Formation, an important exploration target in the Termit Basin, is a typical sandstone hydrocarbon reservoir. This paper used core samples, wireline logs, and seismic data collected in the Dibeilla prospect to determine the impact of oil occurrency on reservoir quality. Cores were analyzed based on thin sections, scanning electron microscopy, X-ray diffraction, and a range of pre-stack inversion modeling approaches by integrating wireline logs to seismic data. Distributions of all potential influencing factors on porosity and permeability were quantified, assessing the influence of all potential controls on the quartz cement. Precise oil saturation of each sand group has been determined using the outputs pre-stack inversion. The main authigenic minerals are quartz overgrowth and clay minerals, which occur as pore-filling and pore-lining cements, reducing porosity and permeability. Quartz overgrowth occurs with varying frequency on both sides of the study area throughout the diagenetic history. The high occurrence of quartz overgrowth in the northern part containing mainly water reservoirs, and the low occurrence in the southern part containing mainly oil reservoirs, indicates that quartz cementation was inhibited by oil emplacement in these facies and is with significant control on porosity and permeability preservation. Reservoir quality in the Dibeilla prospect is primarily determined by a combination of microcrystalline quartz controlled by depositional facies with dissolved secondary porosity and early oil emplacement. Results demonstrate the robust application of combining diagenesis and seismic inversion in predicting favorable reservoirs, useful in reducing exploration risk in undrilled areas and oilfields with similar geologic settings.***

Keywords: Reservoir simulation, sandstone diagenesis, quartz cement, oil effects, reservoir quality, Dibeilla prospect, Niger

1. Introduction

Located on the eastern margin of the Agadem block, the Dibeilla prospect covers an area of about 796 Km^2 and is situated in the structural belt of the Aragagraben and at the northern end of the Fana fault-step zone (**Figure 1**). It is one of the most oil-rich fields of the ongoing producing Agademblock, which is part of the Termit basin in eastern Niger. The latter ispart of the West African Rift System, which developed during the Early Cretaceous breakup of Gondwana and the opening of the South Atlantic and Indian Oceans [1-4]. The oils recovered to date are in the sand deposits of the Eocene Sokor1, which reaches a thickness of 300 to 900 m in [5]. During burial, the deposited sand in these reservoirs never retains its original porosity, texture, mineralogical composition, or even the flow rate as it becomes sandstone. Since a petroleum deposit has been discovered in this sandstone, it is critical to gain the fullest possible understanding of the reservoir quality to support subsequent exploration and evaluation efforts.

The evolution of reservoir quality can be directly linked to diagenesis, as it involves all the changes that sediment undergoes after deposition and before the transition to metamorphism. It is important to understand in detail the multiple processes that fall under the term diagenesis, such as chemical, physical, and biological processes [6], in order to examine what controls the quality of the reservoir. These processes include compaction, deformation, dissolution, cementation, authigenesis, replacement, recrystallization, hydration, bacterial action, and the development of concretions. During these processes, massive chemical and textural reorganization occurs in sandstones and mudstones when detrital grains and the rock textures defined by the grains are lost through reactions with pore fluids. Therefore, predictive models for the evaluation of porosity and permeability at depth depend on understanding these processes and the fluids with them. Asa predictive geophysical method, pre-stack inversion can provide more information about the reservoir and improve accurate reservoir characterization. Pre-stack inversion based on extended elastic impedance (EEI), as described by Whitcombe et al. [7], is playing an increasingly important role in exploration and development of the reservoirs because of its multi-information and high accuracy. The data input for a pre-stack inversion project typically consists of a series of wells, containing P-sonic, S-sonic, and density logs; optional check shots, formation markers, and deviation surveys; a series of interpreted horizons; and seismic offset or angle gathers. It also includes generated volumes of P-impedance, S-impedance, and Vp/Vs ratio. By combining seismic data, log data, and geological interpreted results, the EEI technique, which takes advantage of the fact that log data have high vertical resolution and seismic data have good lateral continuity, can relate elastic parameters such as Poisson's ratio, Lamé coefficients, shear modulus etc., to petrophysical (porosity, permeability, water saturation, shale

volume, etc.) and physical properties (effective rock pressure, grain size, pore distribution, etc.) of the reservoir. Through this linkage, the texture, mineralogy, and fluid content of the reservoir rock can be evaluated. The current study aims to investigate the impact of oil in place on the quality of sandstone reservoir in the Dibeilla prospect and to predict favorable reservoirs in the targeted strata of the basin. This requires a quantitative understanding of:

1) What mineral cements occur in my reservoir, how are they distributed and what is their impacts on porosity and permeability?
2) What events control reservoir quality?
3) Has oil in place had any discernible impact on reservoir quality?

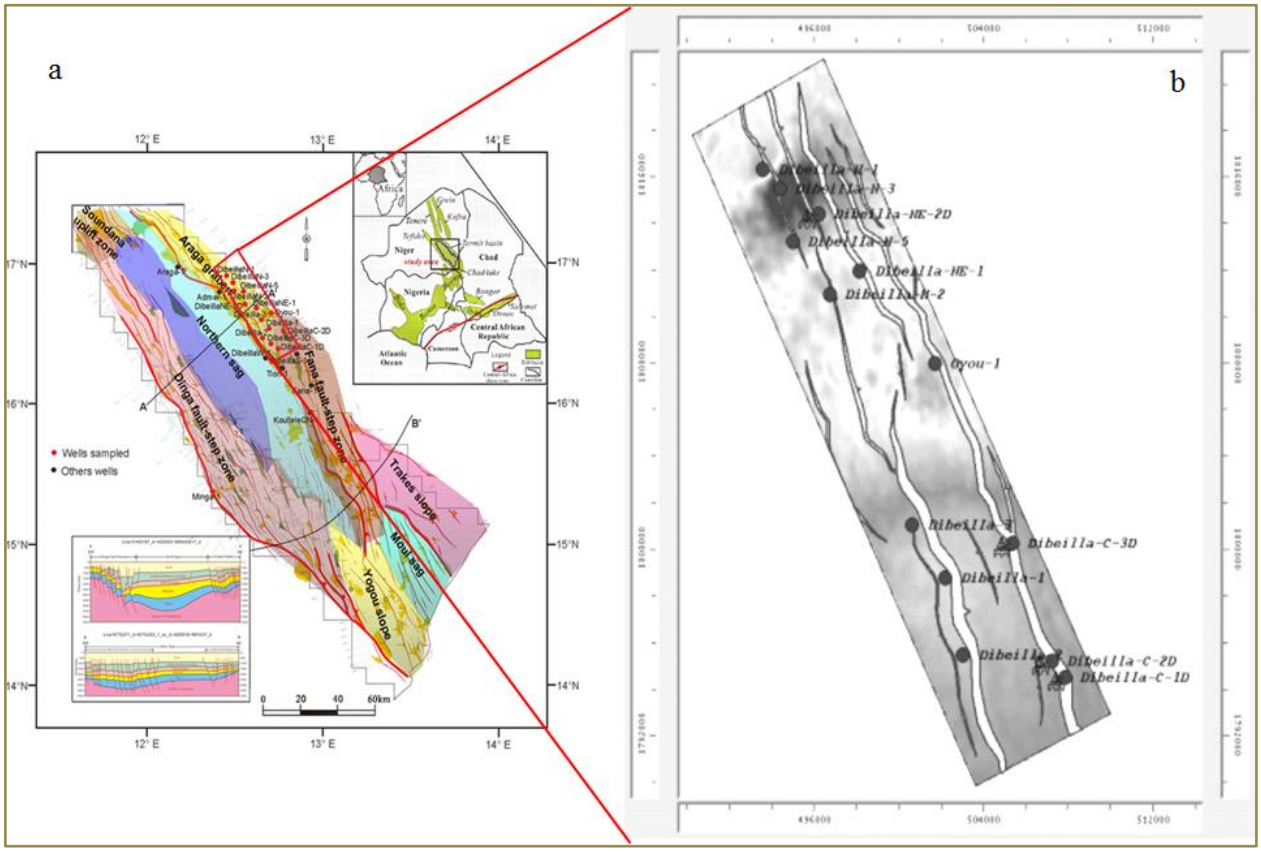

Figure 1: Location map of the study area (**a)** structural units' map of Agadem block, Termit basin, (**b)** structural map of Dibeilla prospect, showing location of studied wells.

2. Geological setting

The formation and development of the Termit Basin is closely related to the evolution of the African Plate, in particular to the development of the Central and West African Rift System (**Figure 1a**) during Early Cretaceous. Tectonic evolution in Termit basin may undergo three phases of syn-rifting, one pre-rifting and one post-rifting [4, 8]. The first episode of intense fault subsidence, initiating the first two syn-rifting phases of the Termit basin, resulted in the development of a series of en-echelon faults toward NW-SE. With rapid subsidence along these NW-SE faults, terrestrial sandstones and mudstones of thousands of meters were formed [9-11], including Lower and Upper Cretaceous formations (**Figure 2**). At the end of Cretaceous, sea level dropped as the African-Arabian Plate was uplifted regionally [12], and the thick Madama fluvial sandstone was deposited in the Termit basin (**Figure 2**). The second episode of intense fault subsidence, triggered by the collision of the African-Arabian Plate with the Eurasian Plate [13], occurred in the Paleogene and superimposed the third syn-rifting phase in the Termit basin. During the deposition of the Sokor1 and Sokor2 formations (**Figure 2**), numerous faults striking NNW-SSE and reactivated NW-SE trending one's were formed.

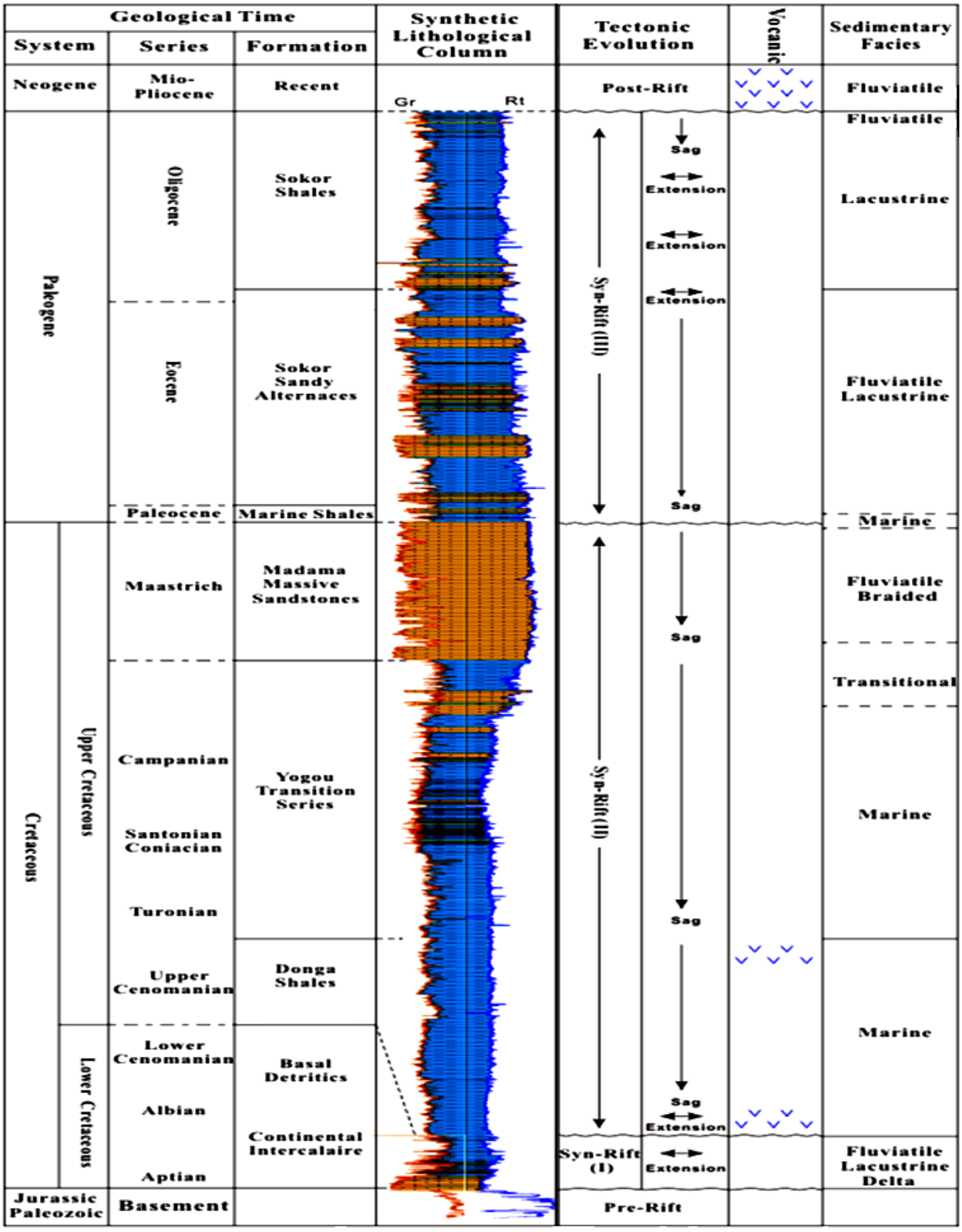

Figure 2: Stratigraphic column of Agadem Block, Termit basin

3. Methods

The main data used for this study came from 13 drill holes distributed across the oilfield of Dibeilla prospect (**Figure 1**). Thirty-two sandstone samples from different sand groups collected in the oil leg and water leg were impregnated with blue or red epoxy resin prior to thin sectioning to indicate porosity. Quantification of detrital and diagenetic components and textural modal grain size and sorting parameters were determined by counting 300 points in each thin section examined under the polarizing microscope. Whole rock analysis of the sandstone samples was also performed by scanning electron microscopy (SEM) at 20 kv using a Cambridge Stereo scan 240. This analysis allowed the identification of the different clay minerals, the determination of the pore structure, type of cements and its mode of occurrence in the pore spaces of the deposit. To identify the clay minerals in the fraction less than 2 µ min

size, which was separated from bulk samples by settling in a water column, X-ray diffraction (XRD) was performed using standard procedures, and quantitative estimates of mineralogy were obtained using methods described by Schultz [14]. Using the 2-theta method described by Moore and Reynolds [15], the proportions of smectite and illite in the illite/smectite (I/S)mixed-layer were determined. The borehole data used are a series of composite logs, including gamma ray (GR), resistivity (LLD and LLS), sonic (DT), density (RHOB), neutron (NPHI), spontaneous potential (SP), and litho-density log. A 3D seismic volume and vertical seismic profile (VSP) are also used.

Rock physical parameters (Vp, Vs and ρ) of the formation are examined to establish the relationship between the petrophysical data and elastic properties as described by Whitcombe et al. [7]using a computer aid LD-GMax™ software. The LD-GMax™ software is based on fluid substitution model technology and uses the various fluids properties, water saturation, framework, porosity, clay content, density (ρ), acoustic travel time, down hole P-wave and S-wave velocities to produce inverted elastic parameters. The shear wave velocity (Vs) was estimated from the measured compressional velocity (Vp) using Greenberg and Castagna [16]empirical relations for porous rock. Well logs and seismic data are processed to generate new log attributes, namely P-impedance, S-impedance, and extended elastic impedance (EEI) on the one hand, and wavelet and angle gathers extraction on the other. In a second step, a cross-correlation study is performed to determine the best values of the projection angle chi (χ) for a better calibration of the seismic to wells tie, so that the different elastic parameters can be accurately extracted from the EEI analysis. The final step consists of implementing and processing the EEI on the inverted seismic data and interpreting the inversion results. In this phase, new seismic inversion attributes are created for various petrophysical and elastic parameters such as shear modulus, Laméfirst coefficients, etc., to understand and model key reservoir properties, allowing efficient discrimination between different lithologies and their fluid content. The figure 4 below shows a workflow in this approach.

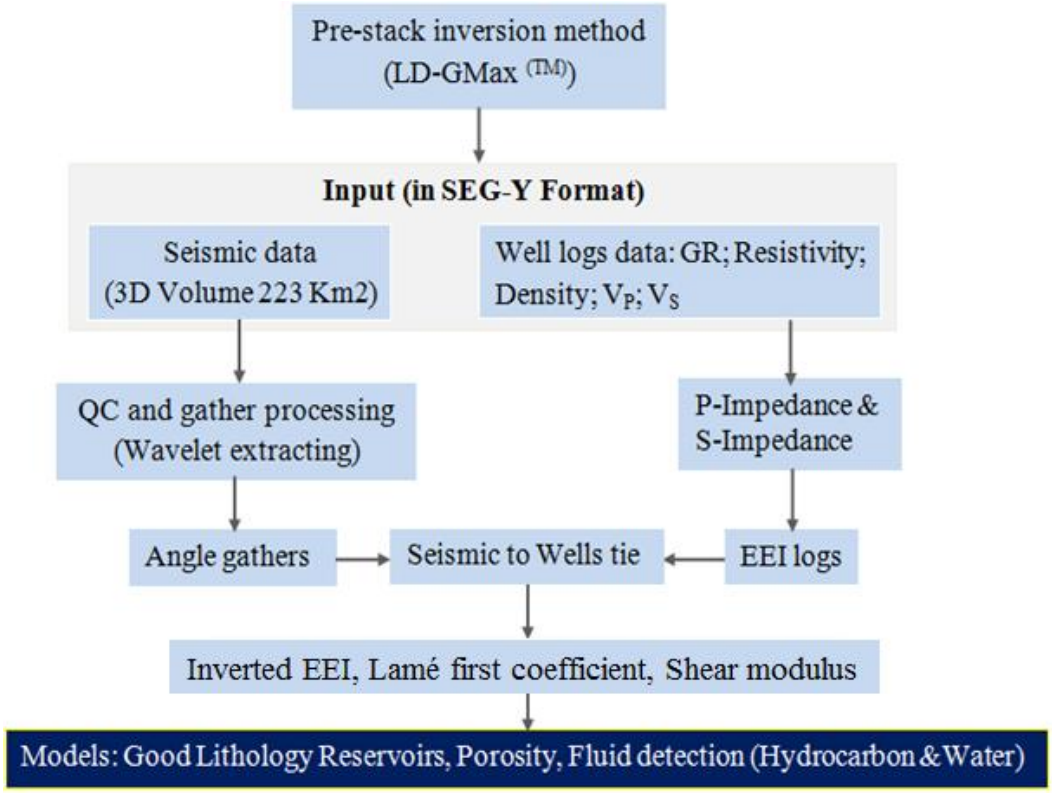

Figure 3: A flowchart showing general method approach

4. Results and interpretations

4.1 Diagenetic processes of Sokor1 sandstone reservoirs

The Sokor1 Formation has undergone numerous diagenetic processes that have great significance for the properties of the reservoir deposit and influence its quality. These processes include compaction, cementation, dissolution, and replacement which have important significance for the sandstone reservoir of the Dibeilla prospect.

The texture of Sokor1 sandstones in the Dibeilla reservoir shows different degrees of mechanical compaction depending on how far the rock has been buried and its content (**Figure 4**). It is mainly a buried diagenesis that leads to physical changes, i.e., after the sediments are burial, as the burial depth increases and under the influence of the overlying gravity and hydrostatic pressure, the water is displaced, then the plastic compositions are displaced into the pores, and the clastic grains line up tightly with concavo-convex and linear contacts (**Figure 4 C and D**). This leads to a reduction in the total volume and porosity of the sediments and thus to a deterioration in the permeability. For the sediments with low content of continental matrix and high content of rigid and coarse well-sorted grains, is mainly characterized by grain contacts after compaction, and the

degree of reduction of primary intergrain pores is low (**Figure 4 B and E; Table 1**). For sediments with a high content of continental matrix and plastic grains, and for sediments with fine grains and poorly sorted, matrix contact mainly occurs after compaction, and the degree of reduction of primary intergrain pores is high (**Figure 4 F; Table 1**). When the matrix content exceeds 15%, rapid compaction and rapid reduction of primary intergrain pores occur.

Table 1: Surface-pore ratio features in thin section of different sedimentary micro-facies in Sokor1 Formation Dibeilla prospect, Termit Basin

Micro-facies	Sample number.	Leg	Distribution range of surface-pore %	Aver. surface-pore ratio %
Distributary channel of delta plain	22	Oil	12-28	**21.9**
		Water	7-21	**15.8**
Underwater distributary channel in delta front	27	Oil	13-35	**24.5**
		Water	9-23	**17.9**
Mouth bar in delta front	19	Oil	10-24	**18.6**
		Water	3-16.5	**11.4**
distal bar in delta front	13	Oil	8-19.5	**16.7**
		Water	2-12.6	**10.8**
Shallow-lake bank bar, Beach bar	14	Oil	2-12.5	**9.5**
		Water	**2-9.6**	**6.2**

Table 2: Assessments of common thin sections taken from Sokor1 reservoirs in Dibeilla prospect Wells'

Samples number	Depth (m)	Sand group	Quartz (%)	Feldspar (%)	Debris (%)	Clay matrix (%)	Calcite cement (%)	Diameter (mm)	Denomination
4	1212-1259.5	E1	84.1	>1	>2	12.3	1	0.05-0.14	Very fine quartz sandstone
6	1334-1342.5	E2	79.97	1	2	14.5	2.8	0.06-0.13	Fine quartz sandstone
4	1468-1470.4	E3	83	1	2	13	1	0.05-0.75	Anisomerous quartz sandstone
6	1492-1525	E4	89.6	<1	<1	8.2		0.12-0.93	Anisomerous quartz sandstone
6	1672-1712	E5	93	<1		6.4		0.13-0.96	Anisomerous quartz sandstone

Table 3: XRD data for whole-rock samples taken from Sokor1 reservoirs in Dibeilla prospect Wells'

Samples number	Depth (m)	Sand group	Relative contents of mineral types (%)							
			Clay contents	Quartz	K- feldspar	Calcite	Dolomite	Rock salt	Pyrite	Siderite
4	1212-1259.5	E1	11.9	82.2	2.9	1	1	1		
6	1334-1342.5	E2	14	78.91	1	2	2	0.72	1	1
4	1468-1478.4	E3	12.5	81.3	0.75			1	0.84	1
6	1492-1525	E4	11.4	84.6	1			0.64		3.4
6	1672-1712	E5	8.2	88.8	1					1.95

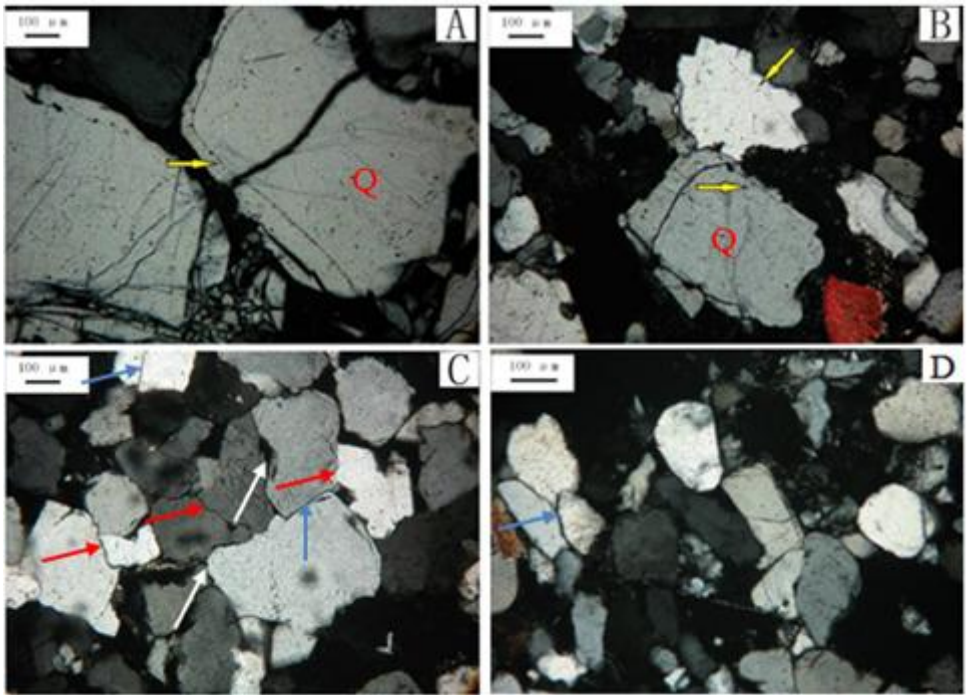

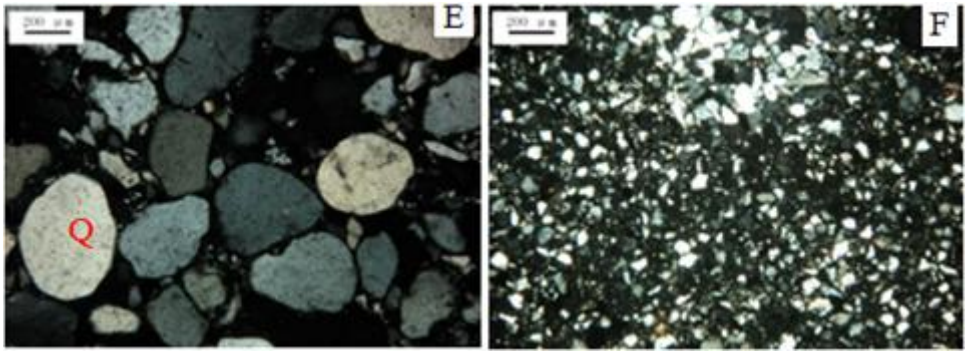

Figure 4: Thin-section photomicrographs of Sokor1 sandstones depicting: (**A)** Coarse grained quartz, micro-fractures, quartz overgrowths (arrow), Dibeilla-N-5, 1432 m, E4; (**B)** Medium grained quartz, quartz overgrowths (arrows), poorly sorted, Dibeilla-1, 1634 m, E4; (**C)** Medium-fine grained quartz, well compacted with suture contacts (red arrows), concavo-convex contacts (white arrows), and long contacts (blue arrows), Dibeilla-2, 1594 m, E4; (**D)** Fine grained quartz, well compacted, oriented compaction, with long contacts (blue arrows), medium sorted, moderately rounded--sub-angular, Dibeilla-1, 1485.5 m, E3; (**E)**Medium grained quartz, point contact, well sorted, sub-rounded--rounded, Dibeilla N-1, 1723 m, E5; (**F)** Siltstone, moderately sorted, poorly rounded, Dibeilla-C-1D, 1375 m, E2

In addition, chemical compaction occurs, which is locally caused by the intergranular pressure of quartz grains, as indicated by the presence of straight and sutured contacts (**Figure 4 C**). Microfractures in brittle framework grains may occur and solid grains may be fractured and crashed or even transformed into fake matrix (**Figure 4 A**), indicating a high degree of mechanical compaction in these sandstones.

The cementation in the Sokor1 sandstones consists mainly of carbonate, quartz overgrowth, clay minerals, and pyrite. The main carbonate cements are calcite, dolomite, and siderite (**Table2 and 3; Figure 5**). Calcite cements occurred sparsely as pore-occluding cements, which appeared as poikilitopic and patchy calcitein which the intergranular pore spaces are completely blocked (**Figure 5**). The XRD data indicate that the dolomite occurs only in the first two sand groups, whereas siderite occurs with increasing burial depth (**Table 3**).

Siliceous cements occurred in the studied reservoir deposits in the form of quartz overgrowths, which are common in coarse-grained sandstones with large intergranular pores (**Figure 4 A-C and Figure 6**). Quartz cementation did not develop in the sandstone samples with high clay mineral content (**Figure 6 D**), so the presence of quartz overgrowth is controlled by detrital quartz grains. Some authigenic quartz locally contains pseudo-hexagonal to hexagonal terminations (**Figure 6 A and B**) or often grows concurrently with a clay phase (**Figure 4 D)**.

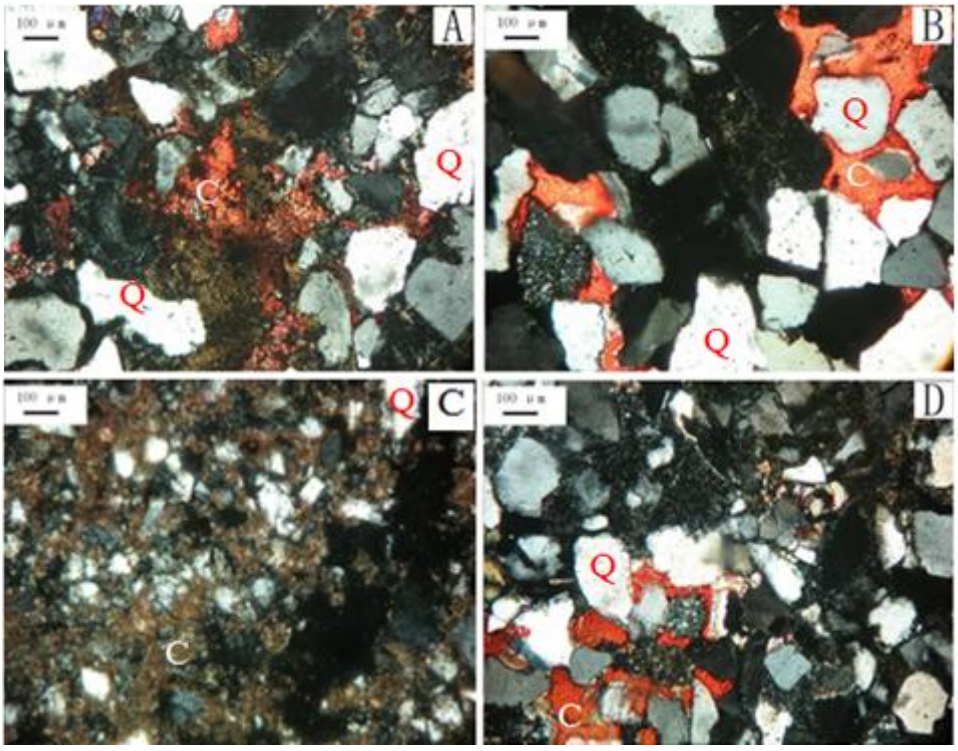

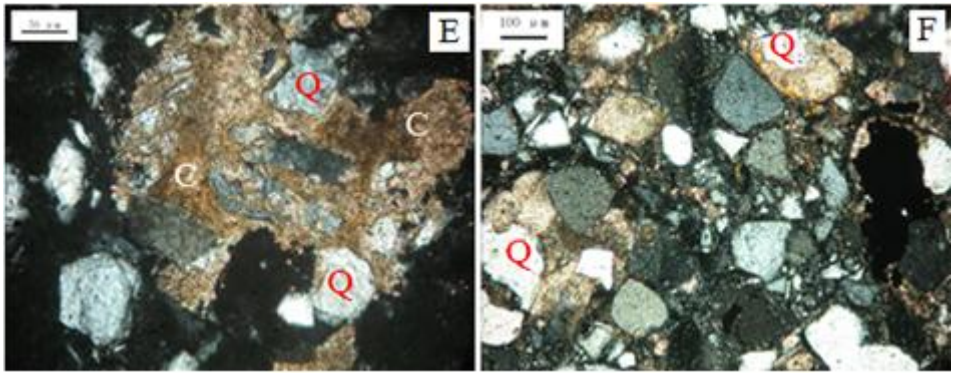

Figure 5: Thin-section photomicrographs of Sokor1 sandstones showing carbonate cements and effects of replacement: (**A)** Patchy calcite reducing pore spaces, Dibeilla N-1, 1253.5 m, E2; (**B)** Poikilitopic pore occluding calcite blocking pore throats, Dibeilla-1, 1315m, E2; (**C)** Patchy calcite reducing pore spaces, Dibeilla-3, 1224.5m, E1; (**D)** Poikilitopic pore occluding calcite blocking pore throats, Dibeilla N-3, 1220m, E1; **(E)** medium-grained quartz with calcite alternates quartz grains, Dibeilla-2, 1352.5m, E2; (**F)** fine-grained quartz with calcite alternates quartz grains and matrix, Dibeilla-N-3, 1310.9 m, E2

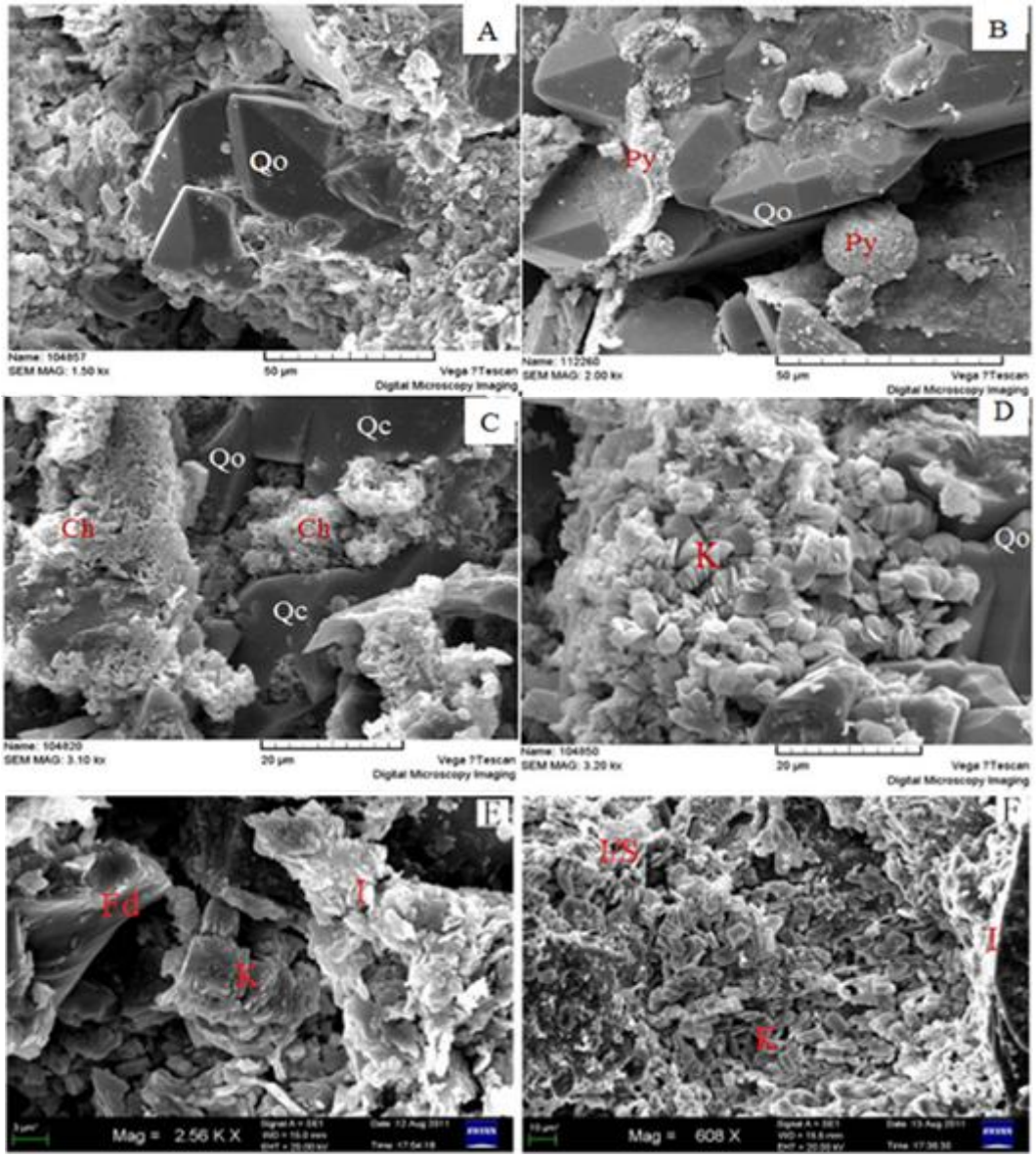

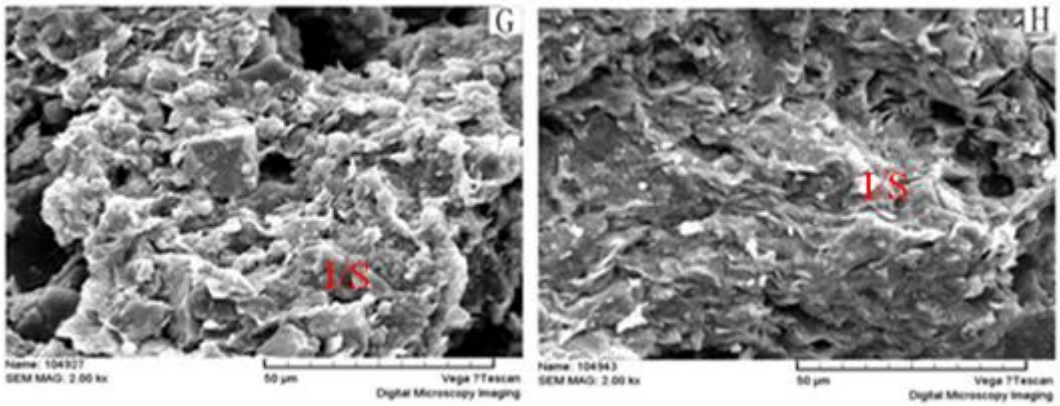

Figure 6: SEM images of quartz overgrowths consisting of small euhedral crystals locally developed in primary pores: (**A)** Dibeilla N-3, 1614 m, E5; (**B)** Dibeilla NE-2D, 1294 m, E3 (**C)** Dibeilla-1, 1315 m, E2; **(D)** Dibeilla-1, 1482 m, E3 (note pore-lining chlorite and pore-filling kaolinite developed in intergranular pore and coated detrital grain); and clay minerals occluding pores: (**E)** Kaolinite occurring as replacement of feldspar due to dissolution of the latter and dissolved pores with its transform into mat-like illite, Dibeilla-2, 1622 m, E4; (**F)** Intergranular pore occluding Kaolinite transform into fibrous illite and mixed-layer illite/smectite (I/S), Dibeilla-3, 1630 m E4; **(G)**Honeycomb-like grain-coating I/S with relic pores, Dibeilla-N-3, 1752 m, E5; (**H)** Honeycomb-like grain-coating I/S and a large amount of micro-pores, Dibeilla-NE-2D, 1410.5 m, E3

Table 4: X-ray diffraction data for clay fraction in samples taken from Sokor1 reservoirs in Dibeilla prospect Wells' (Note: K = Kaolinite, C = chlorite, I= illite, I/S = illite/smectite, S = smectite)

Samples number	Depth (m)	Sand group	Relative contents of clay minerals type (%)					
			K	C	I	S	I/S	%S in I/S
4	1212-1259.5	E1	69.51	9.78	2.94		17.77	60.9
6	1334-1342.5	E2	66.42	10.41	3.62		19.55	50.5
4	1408.5-1418.6	E3	61.23	11.08	6.76		21	30
6	1468-1470.4	E3	63.74	12.02	4.23		20	25
6	1637.4-1642.5	E4	52.50	17.05	5.50		25	20
6	1672-1712	E5	50.50	19.90	6.91		22.69	15

Quartz overgrowth in the Sokor1 sandstones is at the level I in southern part of the Dibeilla area (**Figure 4 B and Figure 6 C and D**), whereas it is at level II in the northern part with width of outgrown side of about 10μm and content of up to 5% (**Figure 4 A and Figure 6 A and B**). Pyrite acts as a porosity-reducing cement because it occurs as a pore-filling (**Figure 6 B**), and its content is low and found only in the E2 and E3 sand groups (**Table 3**). When the pyrite microcrystals are polymerized together, they form a pellet with a framboidal shape (**Figure 6 B**).

XRD analysis of the clay fraction of Sokor1 sandstone samples shows that kaolinite is the most abundant clay mineral, followed by chlorite in the Dibeilla sample (**Table 4**). Under the SEM, the clay minerals occur as pore-filling or pore-lining with many relict pores, depending on the type (**Figure 6**). Kaolinites occurred as pore-filling and the grain coatings show vermicular aggregates, booklets texture and columnar, with residual pores between crystals (**Figure 6 D, E, and F**). Chlorite coatings and pore-fillings grow both, on the surface and along the contact surface of the grain in the form of film or rim (**Figure 6 C**). Mat-like and fibrous illite crystals morphology covering the framework-grain (**Figure 6 E and F**)displayed mainly as the pore filling. Mixed-layers I/S show a honeycomb-like texture as pore-lining rims and pore-filling cements (**Figure 6 G and H**). The presence of the mixed-layers I/S in these sandstone samples indicates the transformation effect of the clay minerals, which have different degree on the facies in the two parts of the study area (**Fig 7 and Figure 8**). In the sandstones of the northern part of Dibeilla prospect, the kaolinite content decreases greatly, while the chlorite and illitecontent increases with increasing quartz overgrowth (**Figure 7**). In the southern part of the study area, the kaolinite content increases with depth, while the illite content increases with the increase of the mixed-layer I/S (**Figure 8**).

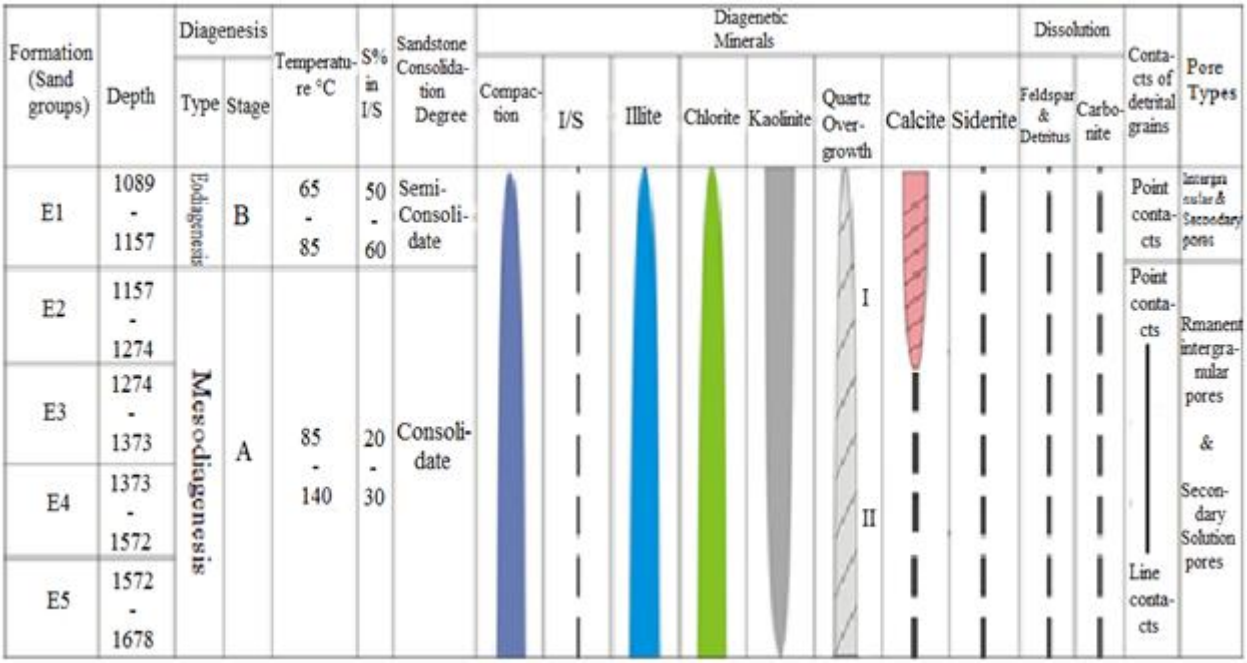

Figure 7: Division of Diagenetic Stage of sandstones in northern part of DibeillaAera, Termit Basin

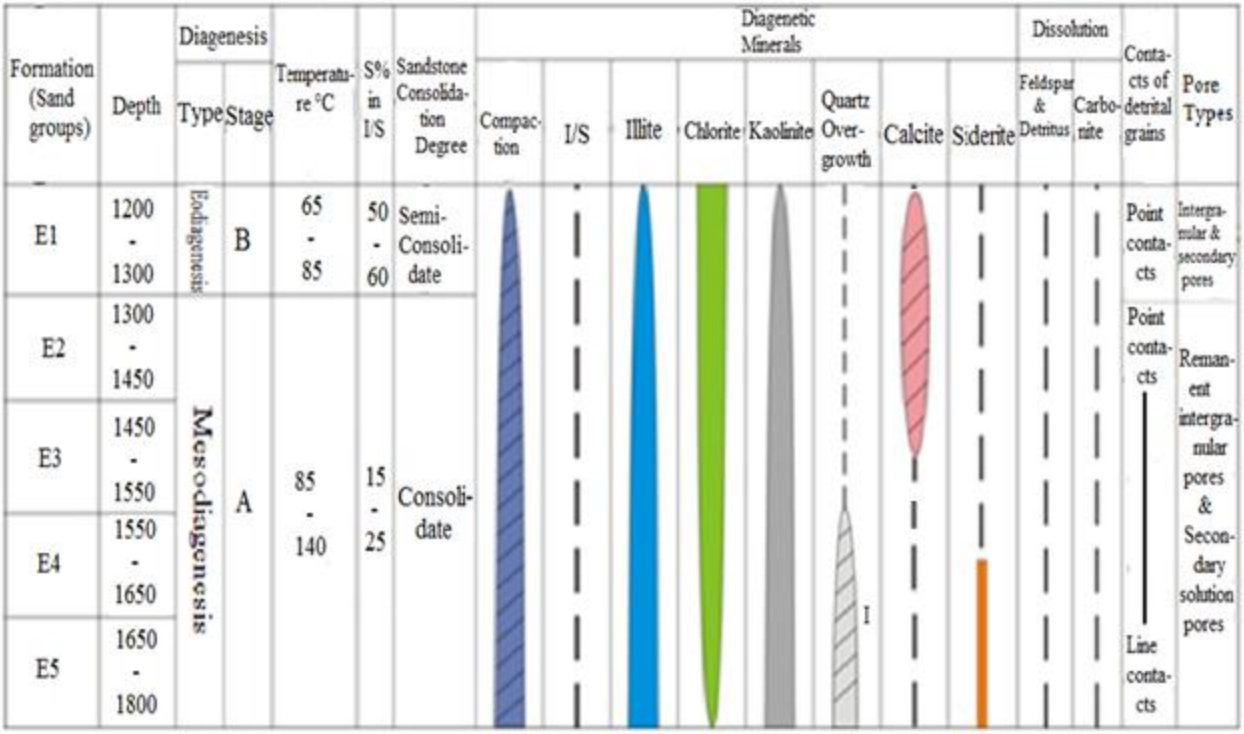

Figure 8: Division of Diagenetic Stage of sandstone in Southern part of Dibeilla Area, Termit Basin

Secondary intra-and inter-pores or mixed pores formed by the dissolution of feldspar grains, quartz grains, and clay matrix in the studied sandstones occur as hull pores or rib-like pores under the SEM (**Figure 9**). In the cast slice samples of the study area, the oversized pores were probably formed chiefly by the complete dissolution of feldspar grains or rock fragments (**Figure 10**). Simultaneous dissolution and precipitation knowing as replacement due to the introduction of foreign materials [17, 18, 19], may affect the porosity to some extent (**Figure 5 C, E, and F**).

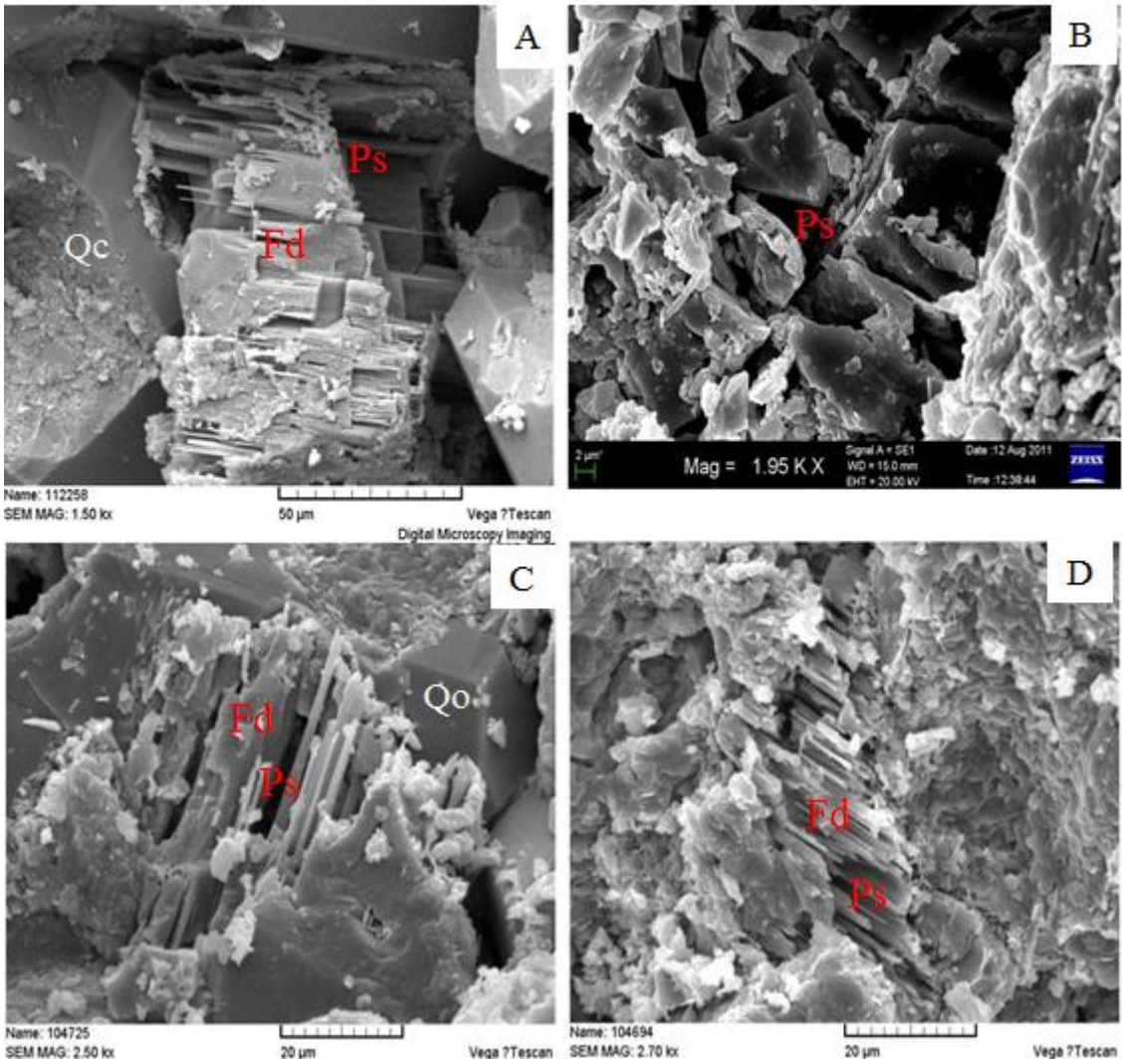

Figure 9: Scanning electron micrographs showing dissolved feldspar and quartz grains (**A)** Cast pores on dissolved detrital feldspar grains, Dibeilla-2, 1240.1 m, E1; (**B)** Intra-pores on dissolved quartz grains, Dibeilla-C-1D, 1502 m, E3; (**C)** Hull pores on dissolved detrital feldspar grains (fenester texture), Dibeilla-1, 1282, E1; (**D)** Rib-like pores on remains feldspar grains (cancellate texture), Dibeilla-N-5, 1192 m, E2

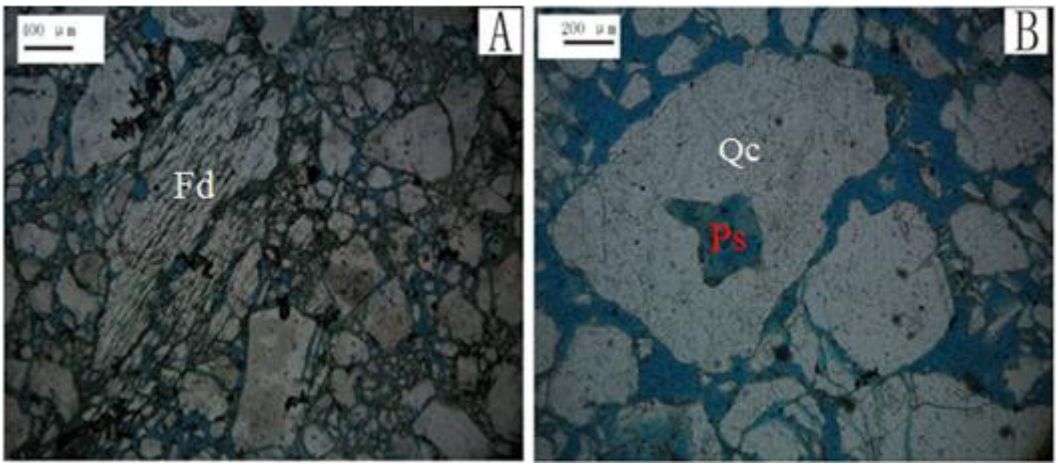

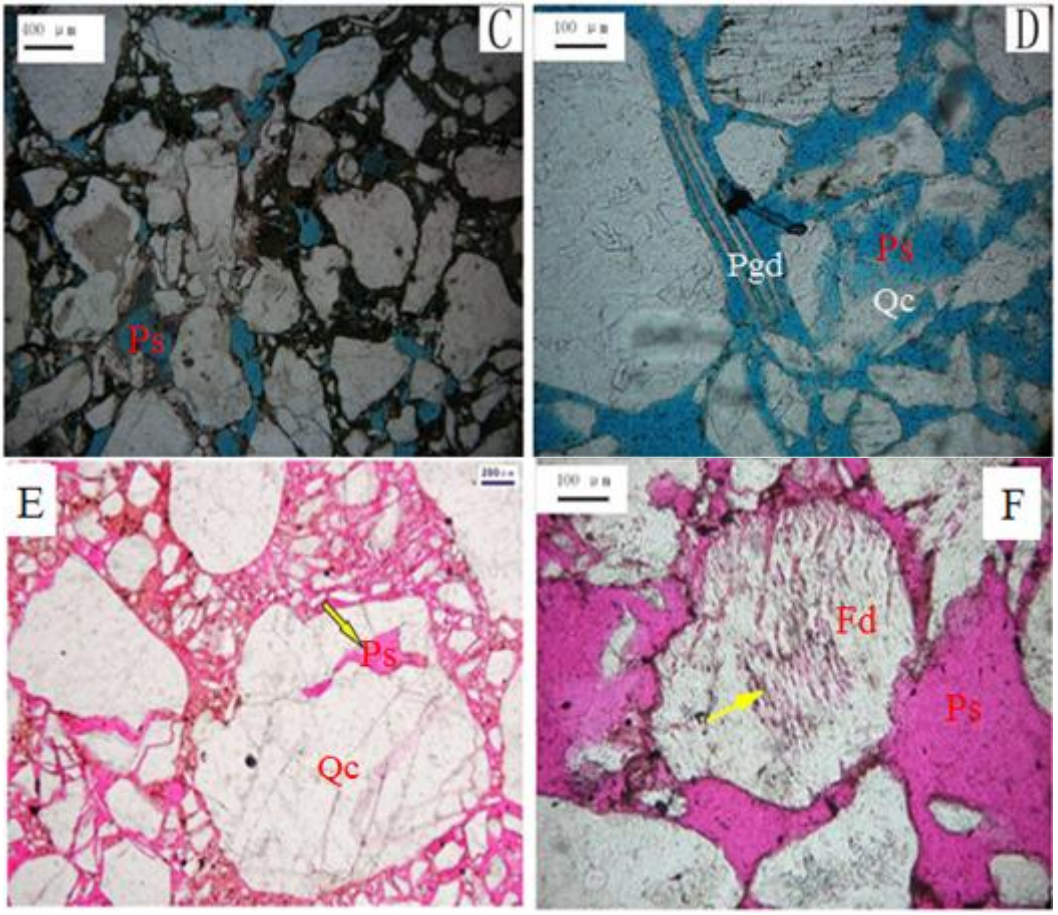

Figure 10: Thin-section photomicrographs showing dissolution and porosity (in blue and red color) (**A)** poorly sorted quartzarenite, dissolved feldspar with intra-grain pores (arrow), Dibeilla-1, 1220.1 m, E1; (**B)** coarse-grained quartzarenite, dissolved quartz with intra-grain pores, Dibeilla-NE-2D, 1245 m, E2; (**C)** medium grained quartzarenite, dissolved matrix with inter-grain pores, Dibeilla-NE-1, 1522.6 m, E4; (**D)** coarse-grained quartzarenite, dissolved mica and quartz with intra-grain pores, Dibeilla-C-1D, 1402.6 m, E2; (**E)** poorly sorted coarse-grained quartzarenite sandstone, dissolved quartz with intra-grain pores, Dibeilla-N-1, 1655.5 m, E5; (**F)** coarse-grained quartzarenite sandstone, dissolved feldspar with intra-grain pores and oversize pores, Dibeilla N-1, 1211 m, E2

4.2. Well logs and inversion results

4.2.1. Well logs interpretation

Based on the processing of the well logs, the porosity and permeability of the target layers are calculate using a pretophysical analysis of rock. Information on porosity is provided by density and sonic logs [20, 21]. **Figure11andTable 5** are the results of the statistical analysis of the target layers of every well in the Dibeilla prospect, showing the mean value of porosity and the histogram of permeability. The results show a high porosity, which is a necessary condition fora favorable reservoir. The mean porosity of every well is more than 20% in the target layer (**Figure 11 a**), which shows that the reservoir belongs to high porosity reservoir. The permeability coefficient indicates the variation in the heterogeneity of the reservoir, which is a important factor affecting the flow rate of oil and gas, indicating the ability of the reservoir to accumulate hydrocarbons [22, 23]. The wells in the southern part of the study area have a high coefficient of heterogeneity of permeability, indicating that their reservoirs are more saturated with hydrocarbons than with water (**Figure 11 b**).

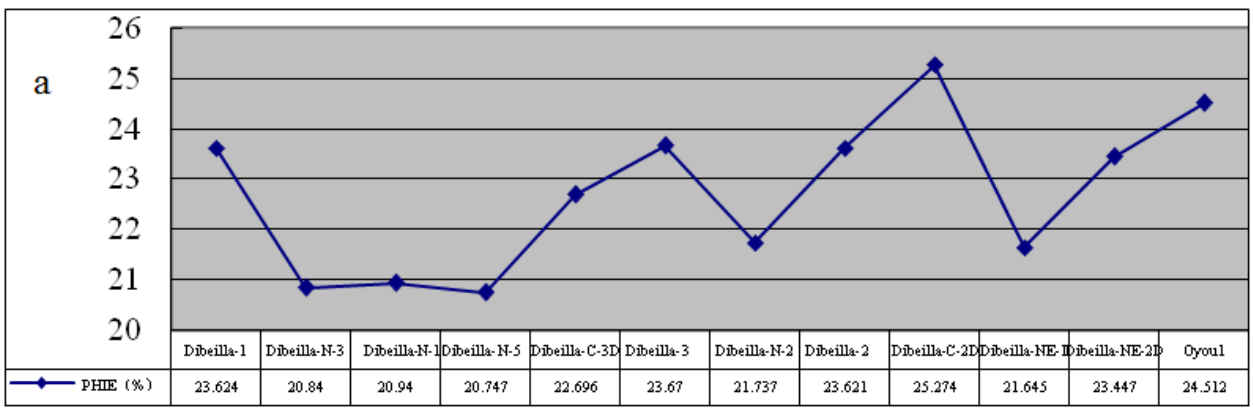

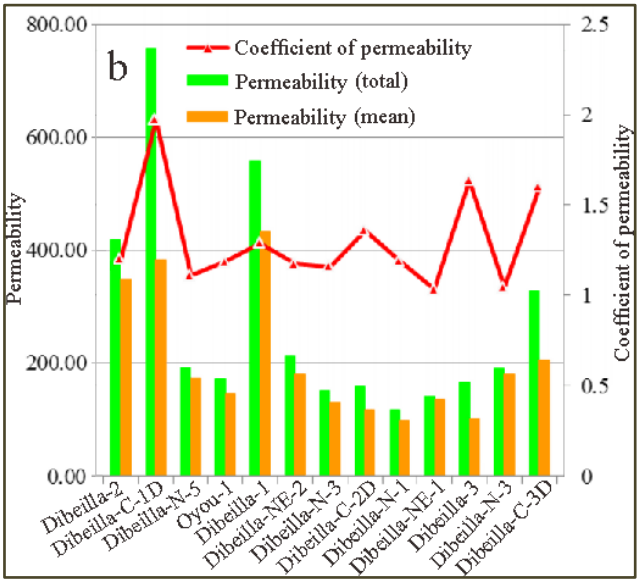

Figure 11 (a): Distribution of mean porosity of single welland (**b)** histogram of permeability in the Dibeilla prospect

Reservoirs in different sedimentary environments (**Table 5**) may have different sedimentary characteristics, such as particle sizes, sorting, and cementation of the rocks, which may directly affect the physical properties of the reservoir formation and the response features of the logging records. An average oil/gas layer may have clear logging response features with resistivity more than three times that in the adjacent water layer (**Table 6**). Therefore, oil saturation (So) is directly related to the porosity and resistivity of a reservoir [24], so (So) can be plotted with porosity and shale content to establish quantitative standards for evaluating oil/gas/water layers. Figure 12 shows the cross-plot of porosity (Φ) and shale content (Vsh) against oil saturation (So), which summarizes the quantitative standards for evaluating such oil/gas/water layers in the Dibeilla deposit, Termit basin as follows: Oil/gas layers have a porosity Φ ≥ 14% and an oil saturation (So) ≥ 45%, whereas water layers have a porosity Φ ≥ 14% and an oil saturation (So)< 45%, with (Vsh) < 35%. On this basis, the compiled results of a typical gas-bearing layer in the Dibeilla-C-3D well (**Figure 13**) show that the shale content is about 10% and the effective porosity is between 28 and 31%. Water saturation (Sw) is less than 10% in these layers of sand groups E2 to E3 with clear mirror-image separation features between density and neutron and a high deep lateral resistivity of nearly 2000 Ωm, indicating oil saturation. Typical oil-bearing strata have low shale content, as evidenced by low gamma-ray and high deep resistivity curves. The density curves often lie to the left of the neutron curves and in mirror-image between them (**Figure 14 and Figure 15**).

Table 5: Categorization and features of sedimentary facies of Sokor1 Formation

Sedimentary facies	Sub-facies	Micro-facies	Basic sedimentary features
Delta	Delta plain	Distributary channels	Coarse sandstone, medium or fine sandstone, oblique bedding, trough cross bedding, flushing-filling structure, charry plant debris.
		natural levee, flood fan	Siltstone, argilaceous siltstone, horizontal bedding, minor wavy bedding, climbing bedding.
		Inter-distributary channels	Argilaceous siltstone, horizontal bedding, bioturbation, plant faults
	Delta front	Underwater distributary channels	Coarse sandstone, medium or fine sandstone, wavy cross bedding, horizontal bedding, worm holes, bio-escape structure.
		Inter-distributary bay	Siltstone, argilaceous siltstone, bioturbation, plant debris.
		Mouth bar	Siltstone, fine sandstone, reverse rhythm with thin lower section and rough upper section, minor cross bedding.
		Distal bar	Argillaceous siltstone, siltstone, horizontal bedding-wavy bedding, bioturbation structure.
Lacustrine	Shore-shallow lake bank bar		Mudstone, very fine sandstone, silty mudstone, shale, horizontal bedding.
	Beach bar		Siltstone, silty fine sandstone.

Table 6: Logging reservoir parameters in the different sandstone intervals of the Dibeilla prospect, Termit Basin in the oil and in the water leg

Sand group	Deep (m)	Gross sand (m)	Net pay (m)	GR (API)	RT (Ω. m)	Φ (%)	PERM (mD)	Sw (%)	Vsh (%)	Result
E1	1239-1243.2	4.2	1.3	35-45	5-7	22	148.2	>70	15	oil-water
	1246.8-1253.8	7	3.8	25	7-20	31	179.7	40	10	oil
	1265.6-1270.7	5.1		15-25	7-23	20	142	100	17	water
	1273.3-1278.8	5.5	2.8	45-65	7-20	24.5	153.5	55	20	oil-water
	1288.6-1308.2	8.3	6.5	15-25	30-110	31	183.6	30	10	oil/gas
E2	1313.1-1316.4	3.3	3	30	15-30	30	210	40	10	oil

	1317.7-1322	4.3	3.6	35	30	30	211.1	45	20	oil
	1321.3-1324.5	3.2		20	11-15	20	158.9	100	10	water
	1320.2-1324.2	4	4	15	200-400	30	215.9	13	10	Oil/gas
	1322.5-1325.8	3.3	3.3	>25	100	27	208.7	30	20	oil
	1326.9-1330.4	3.5	1.9	>30	60	25	212.4	40	20	oil
	1341.9-1348.6	6.7		>40	10-13	21.5	146.7	70	20	water
	1344-1346	2	1.5	45	19	25	198.9	60	10	oil-water
	1370-1376.8	6.7	6.7	15	950-1675	30	223	>10	10	Gas
E3	1396-1398.4	2.4	1.1	>60	20	20	162.3	>70	30	water
	1402.8-1405.8	3	2.8	25	90	30	234	25	10	Oil
	1422-1442	20	16.4	15	60-700	25	219.2	20	15	oil/gas
	1431-1433.2	2.2	2.2	15	1900	28	264.5	>10	10	Gas
	1453.9-1475.3	21.4	9.5	>25	15-100	22.5	198.7	40	10	oil-water
	1489.2-1498.8	3.6		>20	20	21	173.4	>70	10	water
	1502.7-1505.2	2.5	1.5	>50	35	23	204.2	45	10	oil-water
E4	1596.6-1598.6	2	1.8	>60	60	23	375	40	30	Oil
	1599.9-1604.4	4.6	4.6	15	400	30	400.2	10	10	Oil/gas
	1676.5-1688.3	11.8	9.4	>55	30	24	375	30	35	Oil
	1688.6-1692.9	4.3	3.8	>20	8-30	24	368.3	50	10	Oil
	1694.3-1697.5	3.2	3.2	15-20	200	20	227.8	>70	15	Water
E5	1657.1-1673	12.4	11.5	15	400-970	28	438.8	20	10	Oil/gas
	1689.2-1694.6	8.6	4.2	>28	180	23	308.2	30	10	oil-water
	1702-1705	3	2.4	35-45	70	21.5	277.3	>70	20	water
	1774.6-1777.2	2.6	2.2	25	40-60	28	400.4	45	10	oil
	1783.8-1786.5	2.7	1.6	>28	200	26	409.2	15	10	oil
	1789.2-1808.6	8.4	8.2	15	975-1890	31	509.8	>10	10	gas

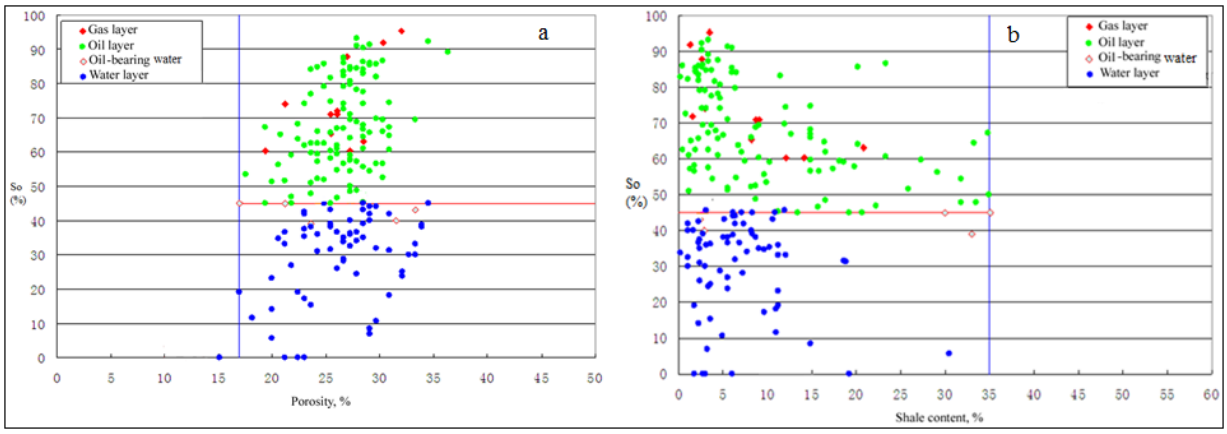

Figure 12: Cross-plots of (**a)**So versus Φ and (**b)** of So versus Vsh in the Dibeilla prospect, Termit basin.

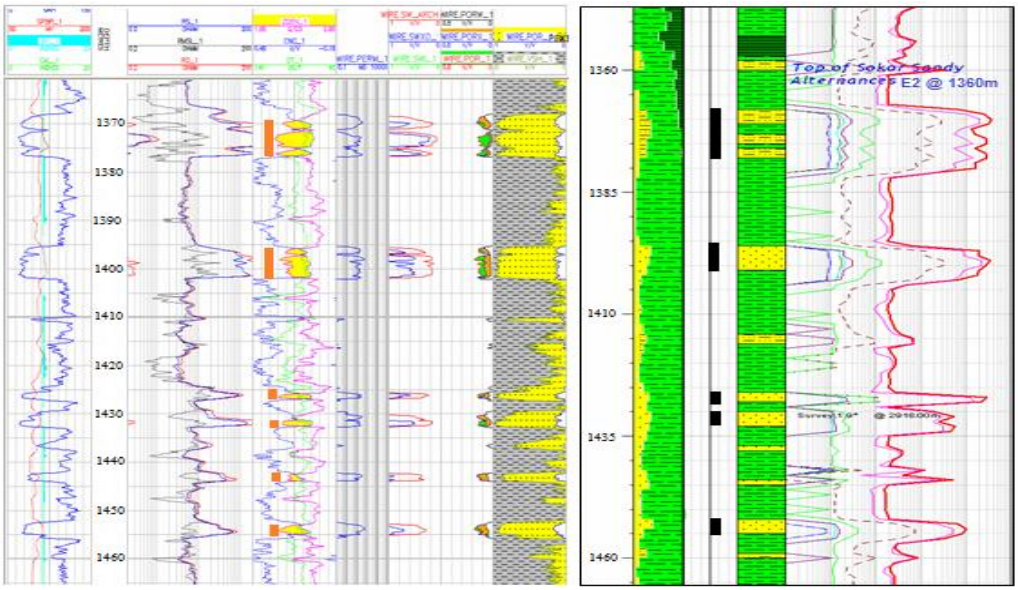

Figure 13: Comprehensive well log interpretation showing typical gas-bearing layers in sand groups E2 to E3 of Dibeilla-C-3D well

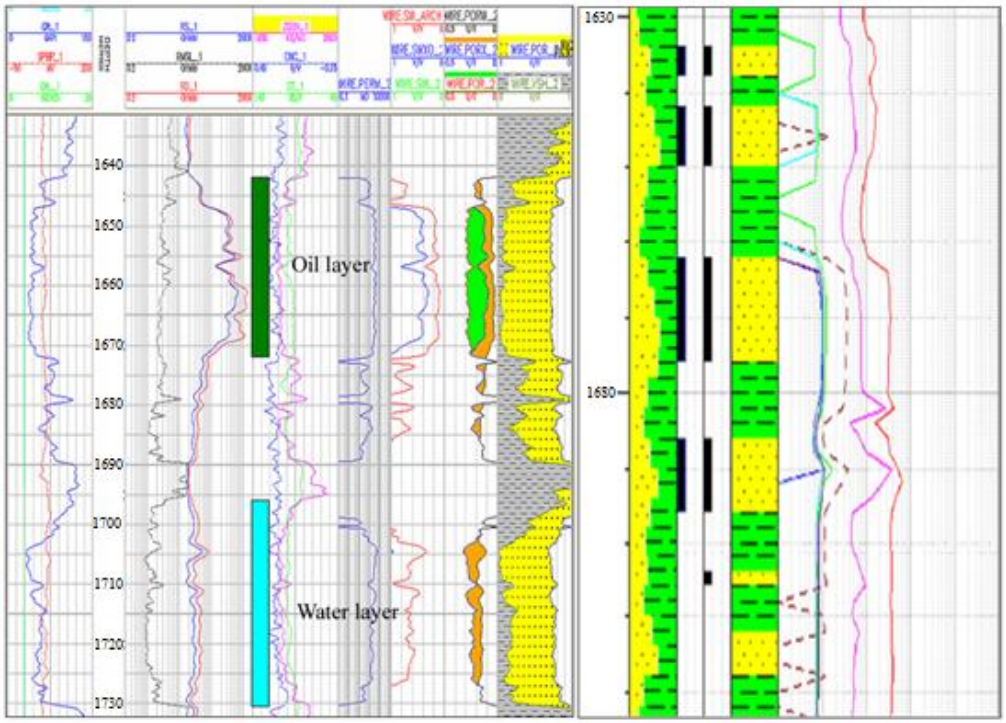

Figure 14: Comprehensive logs interpretation for the sand groups E4 to E5 in Dibeilla-CD-1 Well

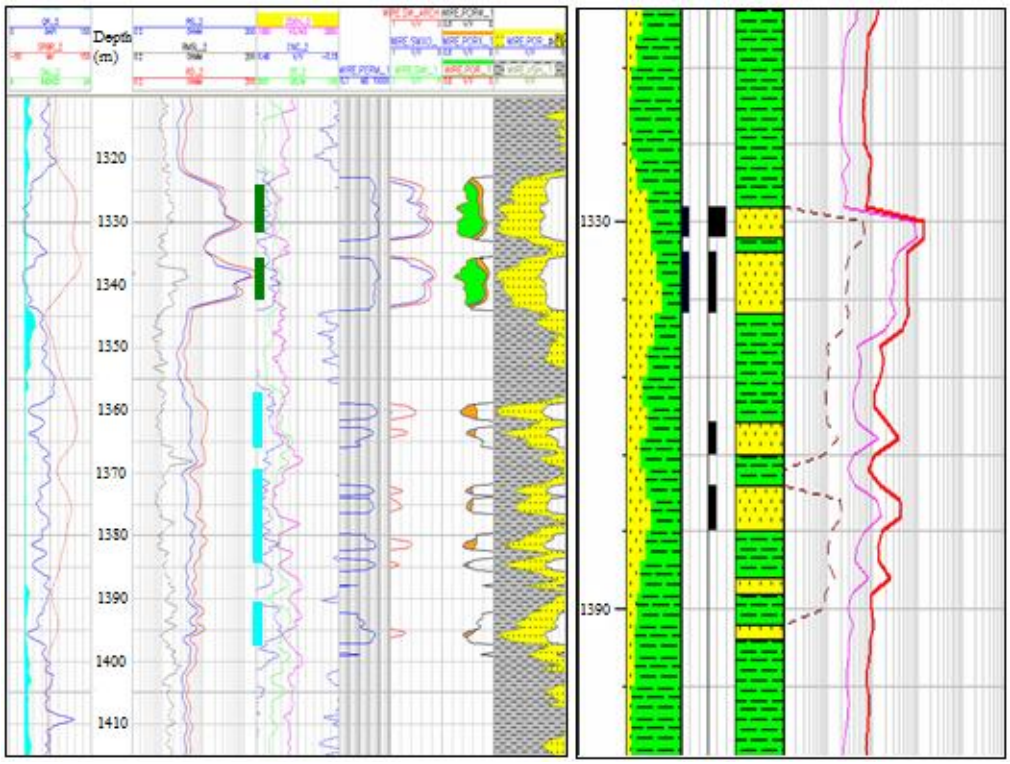

Figure 15: Comprehensive logs interpretation for the sand groups E2 to E3 in Dibeilla-NE-1 well

4.2.2. Interpreted inversion results

Based on the parameter of the effective time window from the gather processing (**Figure 16**) of the 5 sand groups of the Sokor1 Formation, a division of incident angle gathers is made and shown in **Figure 17**. The maximum offset is about 4350 m; the efficient offset is about 2403 m with a maximum depth of the target layer of 1800 m and a maximum incident angle of 34°. The range of divided incident angle is 0-12°, 12-24°, and 24-34° for near, middle and far stack respectively, in which the energy of the target layer is similar, which is basically in accordance with the requirements of seismic pre-stack inversion. Performing pre-stack seismic-to-well tie enables to incorporate shear sonic log in addition to the compressional sonic and density logs to generate elastic impedance logs for each angle-stack.

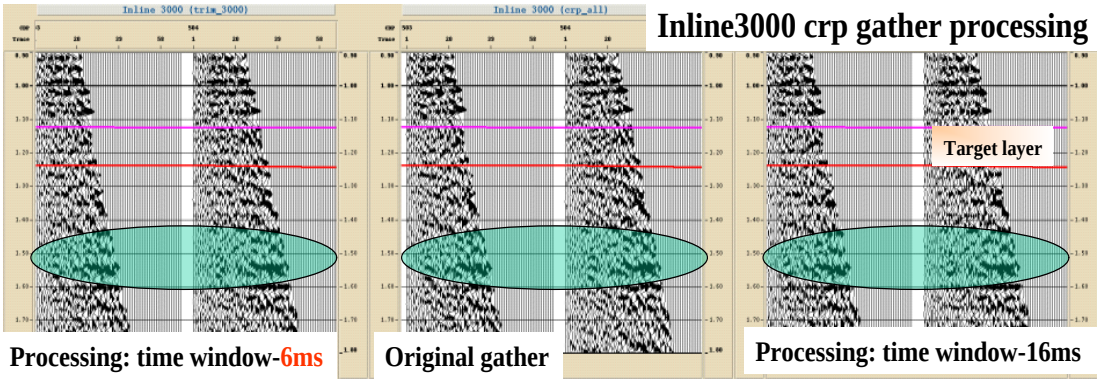

Figure 16: Comparison chart of gather processing shown two-time windows and original gather

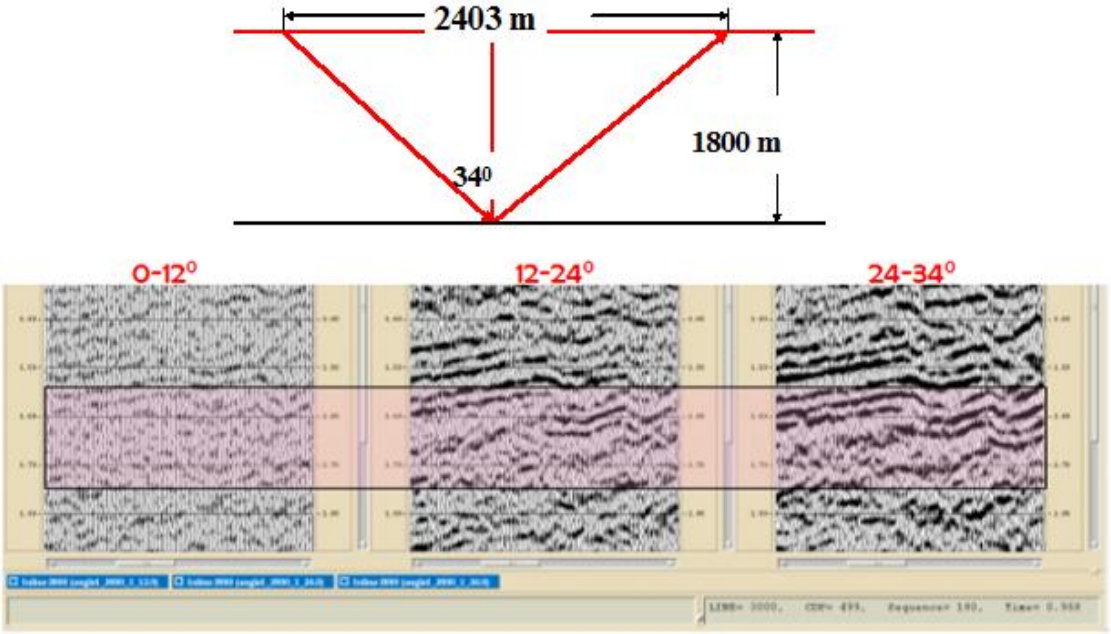

Figure 17: Drawing diagram of maximum incident angle analyses of CRP gather and seismic section corresponding to three angles gather (Near Stack, Mid Stack and Far Stack).

Matching these elastic impedance logs trace with seismic record of nearby wells shows good corresponding time-depth relationships and thus an accurate seismic-to-well tie (**Figure 18**). The generated elastic parameters variation, including extended elastic impedance (EEI), Poisson's Ratio, Shear Modulus and Lamé coefficients correlate with both lithology and the presence of fluids [25-31].

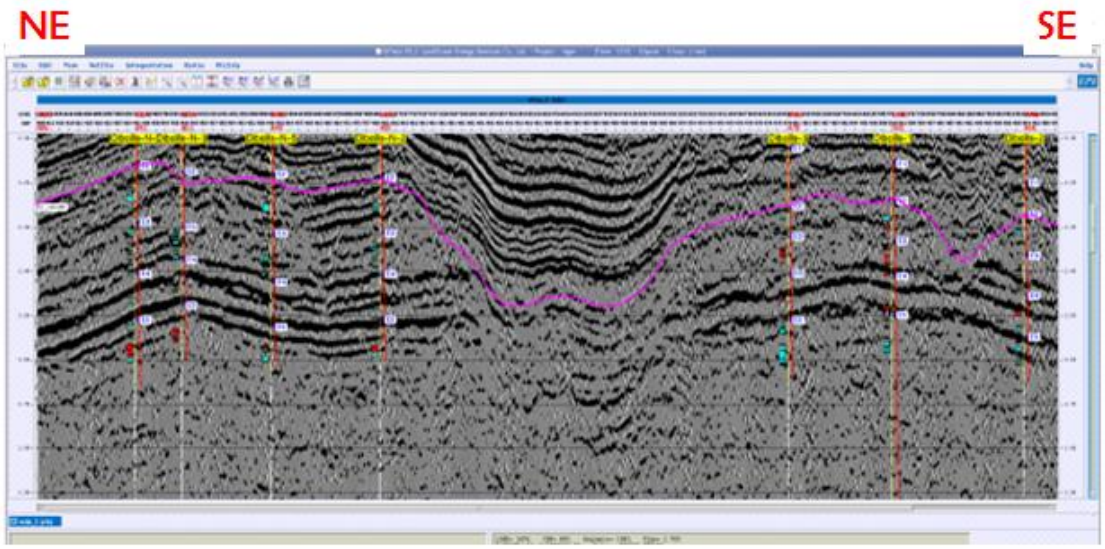

Figure 18: Pre-stack seismic section showing seismic-to-well tie crossing wells Dibeilla-N-1, Dibeilla-N-5, Dibeilla-N-2, Dibeilla-3, Dibeilla-1 and Dibeilla-2

EEI inversion results

The different distribution range of oil/gas layer and water layer can be determined by the well statistics of the extended elastic impedance in the target formation (**Figure 19**). The EEI threshold value between oil/gas and water layers is about 6000 m/s*g/cm3. The value of water layer is basically above 6000 m/s*g/cm3, and the value of oil layer is basically below 6000 m/s*g/cm3 (**Figure 19**).

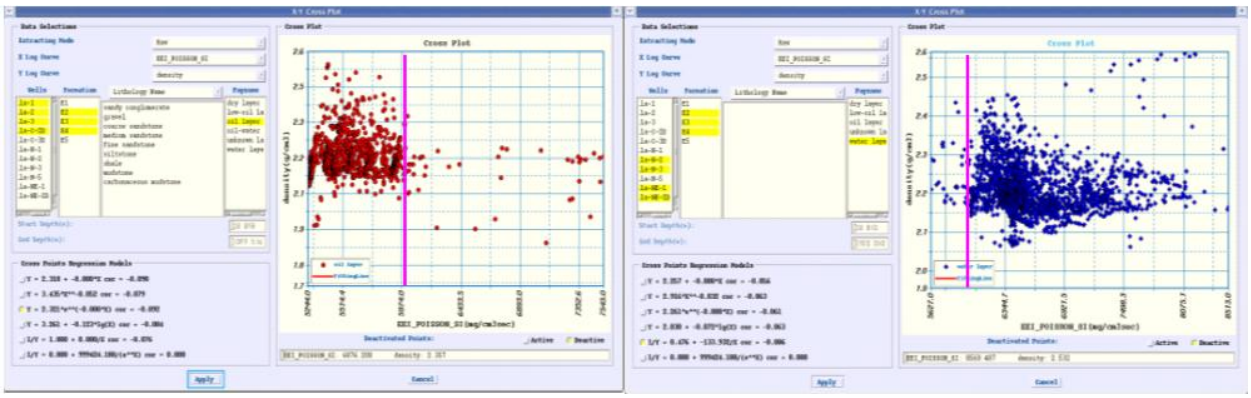

Figure 19: Cross-plots of EEI versus density (**a)**main oil/gas layer at wells interpretation of EEIvalues and (**b)** main water layer at wells interpretation of EEI values.

Therefore, the lower value of EEI generally corresponds to the oil layers and the higher value of EEI generally corresponds to the water layers. Thus, the EEI can reflect the oil-bearing and water-bearing zones at the well location and spatially correlate the same zones in the lateral direction throughout the study area. On this basis, the EEI of oil-bearing reservoir has a relatively lower value than the EEI of water-bearing reservoir, which could be modelled and mapped to distinguish all oil zones from water zones in the process of their identification (**Figure 20and Figure 21**).

The EEI inversion profile shows large differences between the northern and southern parts of the work area (**Figure 20**). Across the wells of the northern part, the high EEI values are the most common, while in to the southern part, the low EEI values are the most common. In addition, the lower EEI values correspond well with the oil reservoirs identified in the log evaluation from the southern part (**Figure 20**). Therefore, most of the reservoirs in the northern part of the study area are water reservoirs (**Figure 21**).

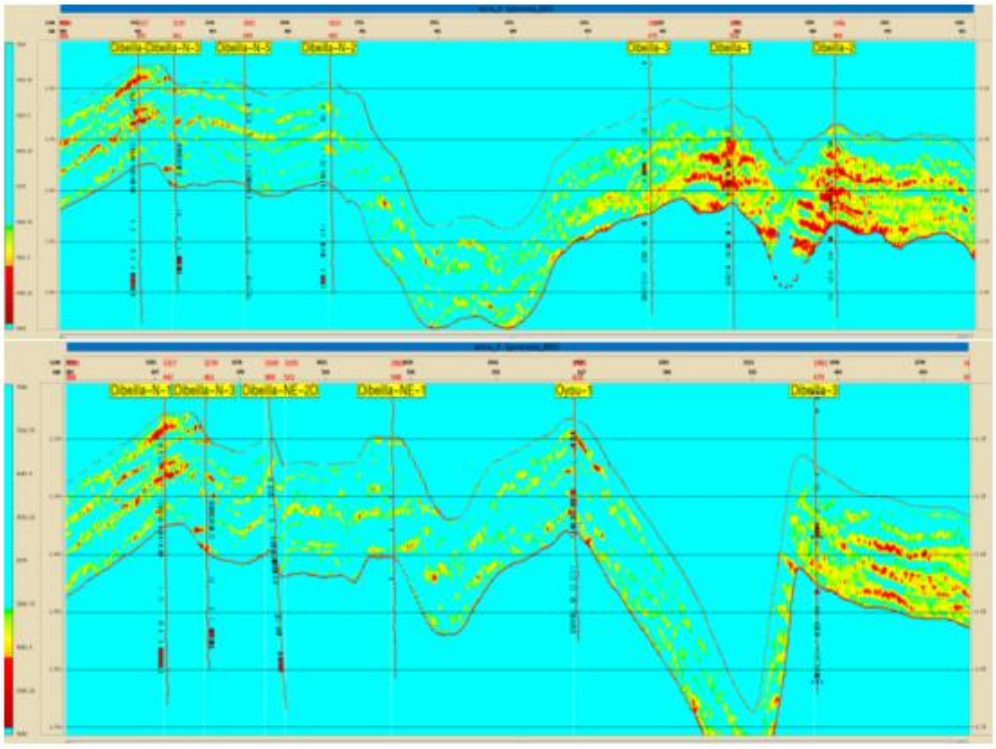

Figure 20: EEI Inversion profile of target layers

Shear modulus inversion results

Shear modulus (μ) is defined as the "resistance to strain that result in a change in shape without a change in volume" [32]. This parameter is very useful for distinguishing lithology and is related to rock matrix [32]. Quartz is the predominant mineral in the sand matrix, so sandstone generally has a higher stiffness than shale and coal, resulting in a higher value of shear modulus than the overlying shale. In addition, the values of shear modulus are directly related to the S-wave velocity, which is known to be close to zero in fluids,

therefore, the shear modulus is low in sandstone containing fluid. Thus, the lower value of shear modulus may reflect a fluid containing layer (**Figure 22 and Figure 23**), indicating a porous lithology saturated with fluid. The profile of the target layers shows that the fluid-bearing layer predicted by the shear modulus coincident with the log interpretation (**Figure 23**), and the coincidence rate can reach up to 90%.

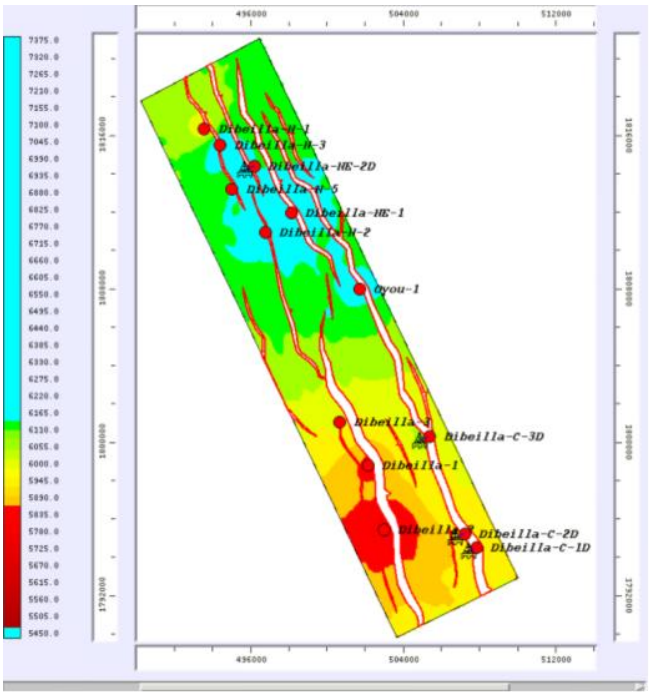

Figure 21: EEI plane map of target layers

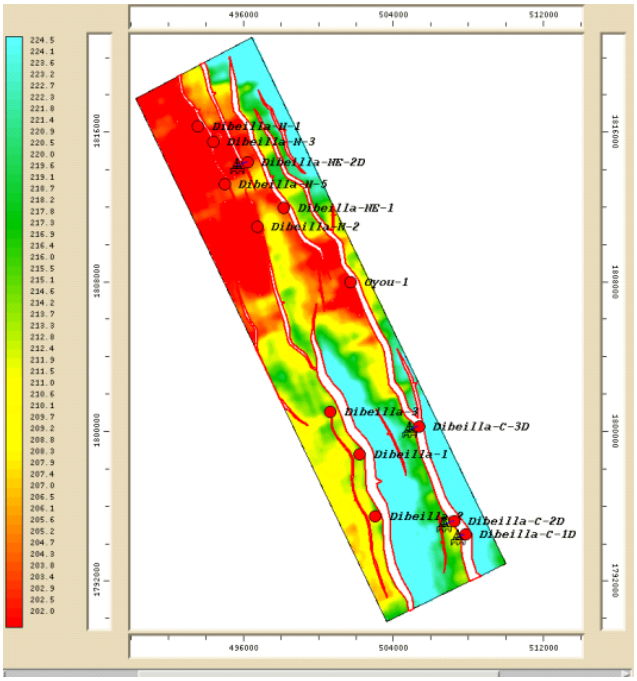

Figure 22: Shear modulus inversion plane map of target layers

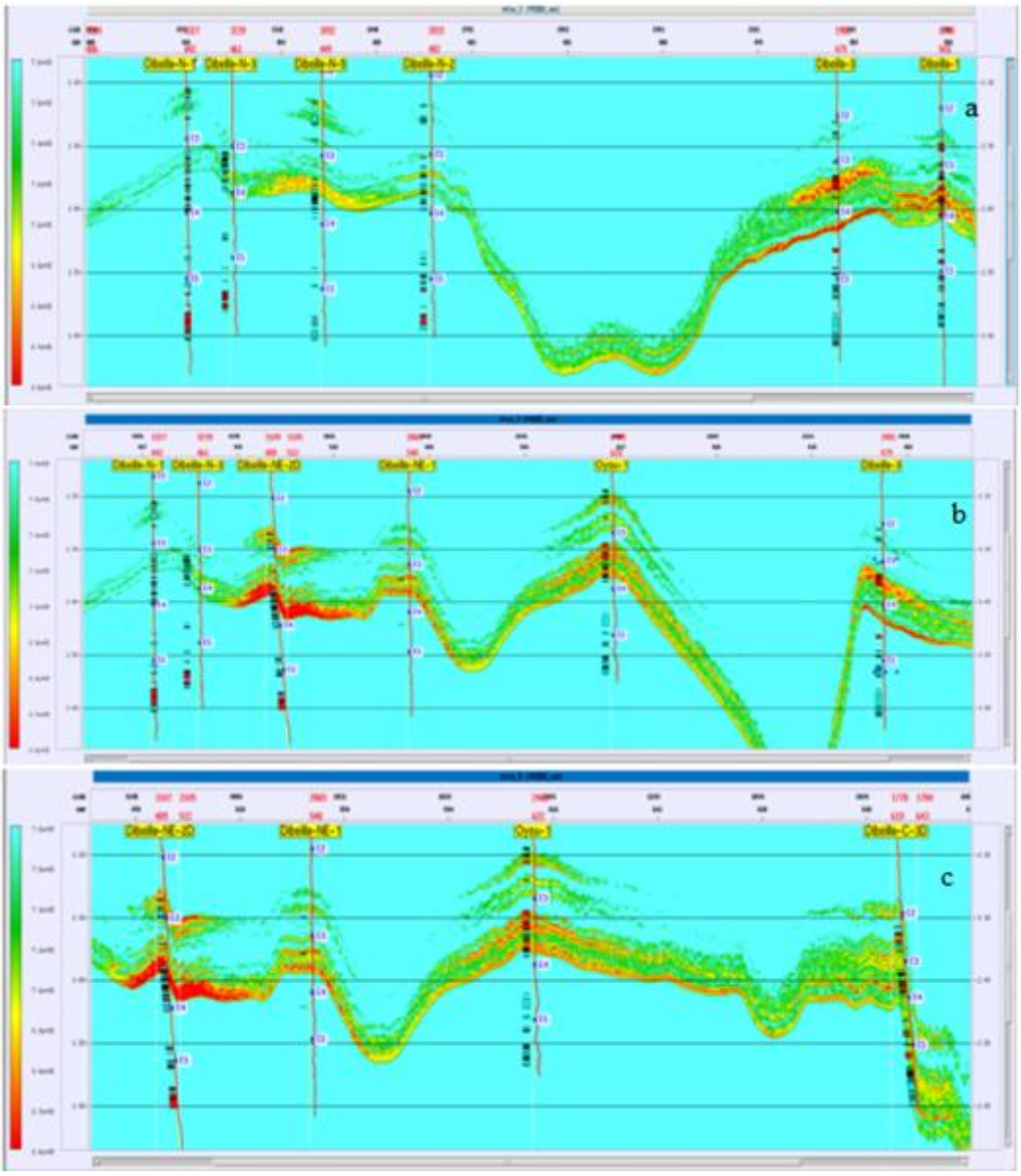

Figure 23: Shear modulus inversion profile of target layers

Lamé's first coefficient inversion results

The first Lamé coefficient (λ) reflects the incompressibility of a medium and is a very useful parameter for distinguishing fluid contents exposed to pore-fluid [32]. λ has close relationship with uncompressed property and is a kind of ability to prevent volume changes due to pressure changes, which makes it sensitive to the presence and change of pore fluids [32, 33]. As a result, the λ value in oily sand reservoirs has low incompressibility values [33]. From the profile of the first Lamé coefficient of the target layers (**Figure 24**), it can be seen that water layers have high sensitivity and their values are higher, while oil layers have lower values.

The plane map of the first Lamé coefficient inversion of the target layers (**Figure 25**)shows a variation in values between the northern part of the study area, where high values are present, and the southern part, which has essentially have low values. In addition, the large distribution of high values of the first Lamé coefficient in the well area near Dibeilla-N-3, Dibeilla-N-5, Dibeilla-NE-2D, and Oyou1is essentially consistent with the log interpretation (**Figure 24**).

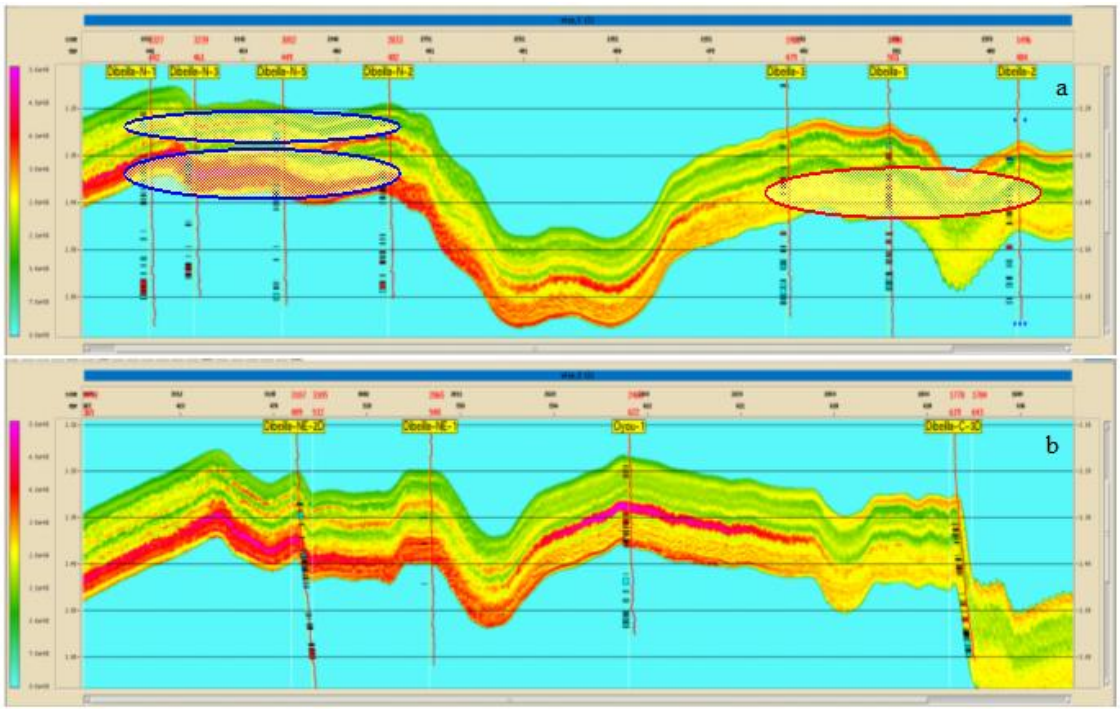

Figure 24: Lamé's first coefficient inversion profile of target layers

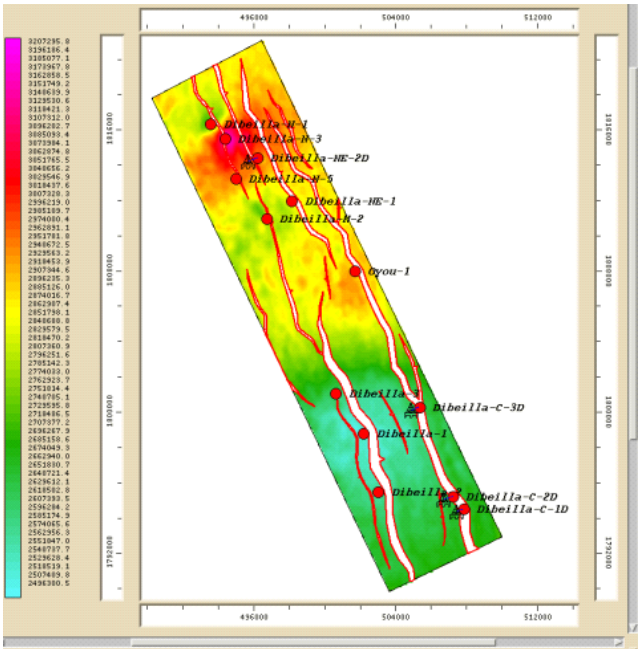

Figure 25: Lamé'sfirst coefficient inversion plane map of target layers

Prediction of favorable oil and gas reservoirs

The combination of the interpreted results of the shear modulus (μ) and the first Lamé coefficient (λ) on one hand, and the shear modulus (μ) with the EEI on the other hand, helps to achieve a new breakthrough in the oil and gas exploration area of the Dibeilla prospect (**Figure 26**). Considering that different lithologies have different rock properties related to fluid content and mineral properties, these are reflected in the elastic impedances. Therefore, in terms of stiffness and incompressibility, oil or gas sand reservoirs should correspond to low λ incompressibility values associated with high stiffness μ of sand grains (quartz). We should keep in mind that μ is not a meaningful and accurate indicator of either oil or water, but of porous lithology, so the combination of λ and μ is a direct indicator of lithology and fluid content [34]. Figure26 (a) shows the results of combining λ and μ, with the predicted result showing the best coincidence with the fluid-bearing reservoir discriminated from log interpretation. From the EEI results, a threshold value separating oil and water layers in different wells, is obtained, which shows that the EEI of the working area can reflect oil-and water-bearing reservoirs. Thus, the combination of EEI and shear modulus can be used to identify the range of these fluid distributions, predict favorable reservoirs, and reduce the variety of prediction methods. Figure26 (b) shows that the oil reservoir potential belt is mainly located in the south of the working area, whereas the water reservoir potential belt is mainly located in the north, except for theDibeilla-N-1 well area.

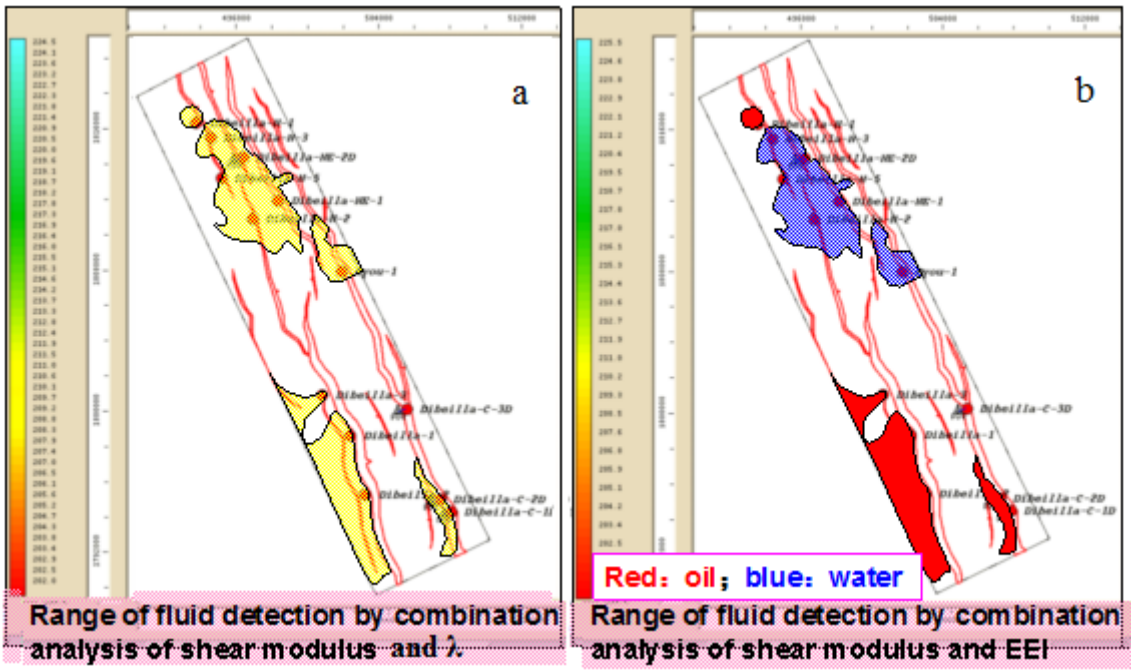

Figure 26: Favorable reservoir plane distribution maps from the combination of (**a)**μ and λ, (**b)**μ and EEI

5. Discussion

The controversial issue of how the emplacement of oil in a reservoir affects the rate of inorganic chemical processes (mineral cementation) is broadly known, as there are two opposing schools of thought. The concept that early emplacement of oil preserves porosity in sandstone reservoirs during diagenesis processes has been discussed in many studies over time [35-53]. In these studies, it was assumed that the displacement of aqueous pore fluids by oil simply halts water-induced geochemical reactions. However, a number of studies have suggested that diagenesis processes can continue freely even after oil is in place, specifically quartz cementation [54-61]. Addressing this controversial question involves the discrimination of the large number of potential factors influencing diagenetic cementation, such as facies, grain size, sorting, clay matrix content, detrital minerals, silica source, pore system properties, distribution of pore-filling cements, and type of fluid saturating the facies. Comprehensive investigations of the Sokor1 sandstones indicate that diagenesis processes differ between the southern part (**Figure 8**), which consist mainly of oil reservoirs (**Figs. 21, 25, and 26**), and the northern part (**Figure 7**), which consist mainly of water reservoirs (**Figs. 21, 25, and 26**), yet samples from both parts belong to the same facies with variable sedimentary features (**Table 5**). The average surface-pore ratio is the highest in underwater distributary channel sand body and mouth bar sand body micro-facies in delta frontsub-facies and in the distributary channel sand body ofthe delta plain in the oil leg (24.5%, 18.6%, and 21.9%, respectively; **Table 1**), whereas it is low in the water leg of the same micro-facies (17.9%, 11.4%, and 15.8% respectively; **Table 1**). The micro-facies of the distal bar in the sub-facies of the delta front and the shallow-lake bank bar and the beach bar of the lacustrine facies (16.7% and 9.5% respectively; **Table 1**) have a lower surface-pore ratio in the oil leg than that of the distributary channel and the mouth bar in the sub-facies of the delta front and the delta plain. The latter consist mainly of coarse sandstones; medium to fine sandstones (**Table 5**) dominated by coarse, medium and fine quartz grains (**Table 3 and Figure 4**), resulting in good reservoir capacity due to quartz grains anti-pressure that laid to the reduction of the intensive diagenetic compaction, thus preserving the original primary inter-grains pores. In addition, the average surface-pore ratios are 10.8% and 6.2% (**Table 1**) in the micro-facies of distal bar of the delta front and in the micro-facies of the shallow-lake bank bar and beach bar of the lacustrine facies in the water leg respectively. In the oil leg as in the water leg, the surface-pore ratio is lowest in the micro-facies of the distal bar, shallow-lake bank bar, and beach bar compared to the micro-facies of the underwater distributary channel and mouth bar in the sub-facies of delta front and delta plain distributary channel. The sand bodies of the former micro-facies, in which porosity is low regardless of fluid content, are characterized by very fine sandstone, argillaceous siltstone, and silty mudstone (**Table 5**). They are therefore dominated by highly clayeygrain matrix, resulting in poor physical properties. In the Sokor1 Formation in the study area, the properties of detrital materials and sedimentary facies are factors that control not only the distribution of the original reservoir space, but also the amounts of original pores and influence the nature and intensity of diagenesis.

Complex diagenetic cementation and migrating fluid content in present-daydeposits of Sokor1 sandstones have altered the original pore types and migration pattern, controlling the final porosity and permeability, which are very important for predicting the reservoir quality. Diagenetic cementation processes are continually active as changes in terms of temperature and chemistry occurred during burial and uplift cycle of the basin history [62]. These processes occurred differently in the two parts of the study area (north and south) in spite of the same temperature variations (**Figs. 7 and 8**). Therefore, the change in the chemistry of the aqueous medium is the most crucial factor influencing cementation in the reservoirs of the Dibeilla prospect. The diagenetic features observed in the studied sandstones, are

the precipitation of authigenic clay minerals (kaolinite, chlorite, illite, smectite/illite), quartz overgrowth, carbonate (calcite) and pyrite, which act as cements for pore-lining, pore-filling, and grain-coating, with different modes of occurrence between water and oil legs, thus strongly affecting reservoir quality. In the northern part of the study area, which is mainly water leg (**Figure 26**), chlorite and illite increase, while kaolinite decreases with increasing of the degree of diagenesis as the sediment is deeply buried (**Figure 7**). In addition, the percentage of smectite in the smectite/illite mixed-layer decreases (**Figure 7 and Tableau 4**), indicating the clay minerals transformation effect due to the change in pore water chemistry as source rocks become mature and release large amounts of organic acids and CO_2. These acidic conditions in the medium favored dissolution of detrital K-feldspar grains (**Figs. 9A, C and D, and 10 A and F**) andillitization of smectite in the interbedded clay, which supply sufficient material (byproducts) that precipitated as quartz overgrowth depending on the wettability of the reservoir. In the water leg (northern part of the study area, **Figure 26**), where the quartz grains are coated with water, quartz overgrowths occur at both diagenesis stages (**Figure 7**). In the oil leg reservoirs (southern part of the study area, **Figure 26**), the quartz grains are coated with oil and prevent the irreducible water to come into contact with the grains surfaces, soquartz overgrowth cement is completely absent at the eodiagenesis stage (**Figure 8**). Moreover, the precipitation of kaolinite increases with depth during mesodiagenesis (**Figure 8**), which occurs as a pore-filling and pore-lining cement, forming a complex pore system with many relict pores and micro-pores between crystallites of kaolinite (**Figure 6 D and E**), exhibiting continuum behavior with increasing irreducible water in the oil leg., Illite increases in the mixed-layer illite/smectite also occurred as a pore-lining and grain-coating exhibited multiple honeycomb-like pores (**Figure 6 F, G, and H**), which favored an addition of irreducible water. Therefore, these oil leg reservoirs with high shale content (**Figure 12**) developed an oil-wetted system that causes some water encountering the grain surfaces, favoring precipitation of quartz cements at level I (**Figure 8**). As oil-wetting increases the tendency of inhibiting dissolution, precipitation and supply rates increase, resulting in greater development of kaolinite (Figure 8), which is more susceptible to oil-wetting than development of quartz cements, which are susceptible to water-wetting behavior [63, 64], indicate the inhibitory effect of oil on quartz cementation. Thus, filling a reservoir with oil thus effectively stops the cementation of quartz overgrowth and thus enhances reservoir quality of the studied sandstones, as quartz overgrow this known to be an important mechanism for deteriorating reservoir quality [65-67. Oil emplacement in the Sokor1 sandstones impedes diagenetic processes and preserves enough pore throats which are conditions for high permeability. The reservoirs encountered by wells in the southern part of the study area (oil legs) have a high permeability coefficient (**Figure 11b**), indicating that the oil in place is a major factor preventing the reservoir storage capacity from being damaged by authigenic cements as diagenetic processes.

Regarding to the reservoir quality, dissolution is the chief master in the formation of secondary porosity in the Sokor1 sandstones. Intra-and inter-granular dissolution pores and some of the oversized pores formed by dissolution (**Figs. 9 and 10**) are an important advantage for the quality of the studied reservoirs. It would also enlarge the primary pores to form mixed pores, which would improve the petrophysical properties of the reservoirs. However, products of dissolved detrital grains, which contribute to the formation of authigenic minerals, often fill the inter-granular pores, especially in the water legs. Reservoir quality is therefore partially improved by dissolution.

6. Conclusion

The Sokor1 Formation is very fine-to coarse-grained deltaic and lacustrine sandstones with an average porosity between 24.5% and 6.5%, depending on whether the sample taken is in the oil leg or water leg.

Apart from compaction, the main diagenetic cements that had an impact on the reservoir quality of the Sokor1 Formation are quartz overgrowths, clay minerals and calcite in the water leg, while in oil leg it is the latter two cements.

Micro-facies with fine-to medium-grained and coarse-grained graded that are grains supported matrix, exhibit high porosity and permeability in the oil leg, with no or very low quartz cementation than the same micro-facies in the water leg.

The diagenetic processes that resulted in secondary porosities (oversized solution pores, secondary intra-and inter-granular pores, and fracture pores) occurred during both diagenetic stages and improve reservoir quality.

Emplacement of oil prior to or during diagenetic processes, has inhibited the growth of quartz cement in Sokor1 sandstones and slowed the rate of supply from dissolution of detrital k-feldspar and quartz grains, which are prone to water-wet behavior and favored the development of kaolinite and chlorite, which exhibit oil-wet behavior.

Acknowledgements

The authors are grateful to the Director General of the “Direction Générale des Hydrocarbures” and CNPC Niger Petroleum S. A., who granted permission to provide data and rock samples. We thank the “Key Laboratory of Tectonics and Petroleum Resources, China university of Geosciences (Wuhan), Ministry of Education, Wuhan, 430074, China’’ for the technical analyses. We appreciate the financial support provided by the UNESCO/People’s Republic of China (The Great Wall) Co-Sponsored Fellowships. Finally, the authors thank an anonymous reviewer whose constructive comments greatly improved the manuscript.

Data Availability Statement: All data, and models used during this study appear in the submitted article.

Declarations

Conflict of interest: The authors declare that they have no known competing financial interests or personal relationships

that could appear to influence the work reported in this paper.

References

[1] Fairhead, J. D. : Geophysical controls on sedimentation in the African Rift Systems. In Frostick, L. E., Renaut, R. W., Reid, I., and Tiercelin, J. J., (Editors), Sedimentation in the African Rifts. Geol. Soc. London Spec. Publ. 25, 19-27 (1986)
[2] Schull, T. J. : Rift basins of interior Sudan, petroleum exploration and discovery. AAPG Bulletin vol. 72, 1128-1142 (1988)
[3] Genik, G. J. : Regional framework, structural and petroleum aspects of rift basins in Niger, Chad, and the Central African Republic: Tectonophysics, 213 (1-2), 169-185 (1992)
[4] Genik, G. J. : Petroleum Geology of Cretaceous-Tertiary rift basins in Niger, Chad and Central African Republic: AAPG Bull., 77 (8), 1405-1434 (1993)
[5] Hamma, A. M., and Harouna, M. : Diagenesis and reservoir quality evolution of the Paleogene Sokor1 sandstones in the Agadem Block, Termit Basin, Eastern Niger. International Journal of Advanced Geosciences, 7 (2), 147-172 (2019)
[6] Worden, R. H., Burley, S. D. : Sandstone diagenesis: from sand to stone. In: Burley, S. D., Worden, R. H. (Eds.), Clastic Diagenesis: Recent and Ancient. International Association of Sedimentologists, vol. 4. Blackwells, Oxford, 3-44 (2003)
[7] Whitcombe, D. N., Connolly, P. A., Reagan, R. L., Redshaw, T. C. : Extended elastic impedance for fluid and lithology prediction. Geophysics, 67 (1), 63-67 (2002)
[8] Maurin, J. C., and Guiraud, R. : Basement control in the development of the Early Cre-taceous West and Central African Rift System: Tectonophysics, 228, 81-95 (1993)
[9] Guiraud, R., Bellion, Y., Benkhelil, J., and Moreau, C. : Post-Hercynian tectonics in Northern and Western Africa: Geological Journal, vol. 22, thematic issue, 433-466 (1987)
[10] Guiraud, R., and Maurin, J. C. : Le rifting en Afrique au Crétacé inférieur: synthèse structurale, mise en évidence de deux étapes dans la genèse des bassins, relations avec les ouvertures océaniques péri-africaines. Bull. Sot. Giol. Fr. 162, 811-823 (1991)
[11] Guiraud, R., Binks, R. M., Fairhead, J. D., and Wilson, M. : Chronology and Geodynamic Setting of Cretaceous-Cenozoic Rifting in West and Central Africa Tectonophysics, 213, 227-234 (1992). https://doi. org/10.1016/0040-1951 (92)90260-D
[12] Guiraud, M. : Late Jurassic rifting-Early Cretaceous rifting and Late Cretaceous transpressional inversion in the Upper Benue basin (NE Nigeria). ElfAquitaine Bull., 17, (2), 371-383 (1993)
[13] Binks, R. M., and Fairhead, J. D. : A plate tectonic framework for the evolution of the Cretaceous rift basins in West and Central Africa. Tectonophysics, 213 (1-2), 141-151 (1992). https://doi. org/10.1016/0040-1951 (92)90255-5
[14] Schultz, L. G. : Quantitative interpretation of mineralogical composition from X-ray and chemical data for the Pierre Shale. Geological Survey Professional paper 391-C (1964) Doi: 10.3133/PP391C
[15] Moore, D. M., and Reynolds, R. C. : X-Ray Diffraction and the Identification and Analysis of Clay Minerals. Oxford, New York: Oxford University Press, 2nd ed. pp. 378 (1997)
[16] Greenberg, M. L., and Castagna, J. P. : Shear-Wave Velocity Estimation in Porous Rocks: Theoretical Formulation, Preliminary Verification and Applications. Geophysical Prospecting, 40, 195-209 (1992). https://doi. org/10.1111/j.1365-2478.1992. tb00371. x
[17] Walker, T. R., 1962. Reversible Nature of Chert-Carbonate Replacement in Sedimentary Rocks. Geological Society of America Bulletin vol. 73, issue 2, 237, Doi: 10.1130/00167606 (1962)73 [237: RNOCRI]2.0. CO; 2.
[18] Fairbridge, R. W., 1967. Phases of Diagenesis and Authigenesis. In Larsen G & Chilingar C. V (Eds.) Diagenesis in Sediments. Elsevier, Amsterdam, 91-125.
[19] Lakshtanov, L. Z., and Stipp, S. L. S., 2010. Interaction between dissolved silica and calcium carbonate: 1. Spontaneous precipitation of calcium carbonate in the presence of dissolved silica. Geo. et Cosm. Acta, Vol. 74, Issue 9, 2655-2664, Doi: 10.1016/j. gca.2010.02.009.
[20] Peters, E. J. : Advanced Petrophysics: Volume 1: Geology, Porosity, Absolute Permeability, Heterogeneity and Geostatistics. Live Oak Book Co, Austin, Texas (2012)
[21] Tiab, D., and Donaldson E. C. : Petrophysics: Theory and Practice of Measuring Reservoir Rock and Fluid Transport Properties. 3rd ed. Elsevier (2012)
[22] Weber, K. J. : How heterogeneity affects oil recovery. In Reservoir Characterization; Lake, B. L. W., Carroll, H. B., Eds. ; Academy Press: Orlando, FL, USA (1986)
[23] Muggeridge, A., Cockin, A., Webb, K., Frampton, H., Collins, I., Moulds, T., Salino, P. : Recovery rates, enhanced oil recovery and technological limits. Philos. Trans. Ser. A Math. Phys. Eng. Sci., pp. 372 (2014)
[24] Archie, G. : The Electrical Resistivity Log as an Aid in Determining Some Reservoir Characteristics. Transactions of AIME, 146, 54-62 (1942)
[25] Ostrander, W. J. : Plane-wave reflection coefficients for gas sands at non-normal angles of incidence. Geophysics, 49, 1637-1648 (1984)
[26] Fjær, E. : Static and dynamic moduli of a weak sandstone. Geophysics, 74 (2): 103-112 (2009)
[27] Gray, D. : Elastic inversion for Lamé parameters, 72nd SEG Annual Meeting, Expanded Abstracts, 21, 213-216 (2002). https://doi. org/10.1190/1.1817128
[28] Gray, D. : Estimating compressibility from seismic data. In 67th EAGE Conference & Exhibition Extended Abstracts, pp. 25 (2005)
[29] Rickman, R., Mullen, M. J., Petre, J. E., Grieser, W. V., Kundert, D., et al. : A practical use of shale petrophysics for stimulation design optimization: All shale plays are not clones of the barnett shale. In SPE annual technical conference and exhibition. Society of Petroleum Engineers, 1-11 (2008)
[30] Goodway, B., Perez, M., Varsek, J., and Abaco, C. : Seismic petrophysics and isotropic-anisotropic avo methods for unconventional gas exploration. The

Leading Edge, 29 (12): 1500-1508 (2010)
[31] Gray, D., Anderson, P., Logel, J., Delbecq, F., Schmidt, D., and Schmid, R. : Estimation of stress and geomechanical properties using 3d seismic data. EAGE, First break, 30 (3): 59-68 (2012)
[32] Goodway, B., Chen, T., and Downton, J. : Improved avo fluid detection and lithology discrimination using lamépetrophysical parameters; "λρ", "μρ", & "λ/μ fluid stack", from p and s inversions. In SEG Technical Program Expanded Abstracts, Society of Exploration Geophysicists 183-186 (1997)
[33] Wasiu, O. R., and Adeoye, T. : Petrophysical Sensitivity of Elastic Modulus and Inverse Quality Factor (1/Q) Analysis in Well Logs. Pacific Journal of Science and Technology, vol. 15 (1), 404-414 (2014)
[34] Hazim H. Al-D. and Alkhafaf S. : Comparison of Kρ and λρ in clastic rocks, A test on two wells with different reservoir-quality stacked sands from West Africa. The Leading Edge 30 (9), 986-994 (2011). https://doi. org/10.1190/1.3640520
[35] Dixon, S. A., Summers, D. M., and Surdam, R. C. : Diagenesis and preservation of porosity in Norphlet Formation (Upper Jurassic), southern Alabama: American Association of Petroleum Geologists Bulletin, vol. 73, 707-728 (1989)
[36] Saigal, G. C., Bjorlykke, K., and Larter, S. : The effects of oil emplacement on diagenetic processes; examples from the Fulmar reservoir sandstones, central North Sea: American Association of Petroleum Geologists Bulletin, vol. 76, 1024-1033 (1992)
[37] Robinson, A., and Gluyas, J. : Duration of quartz cementation in sandstones, North Sea and Haltenbanken Basins: Marine and Petroleum Geology, vol. 9, 324-327 (1992)
[38] Emery, D., Smalley, P. C., Oxtoby, N. H., Ragnarsdottir, K. V., Aagaard, P., Halliday, A., Coleman, M. L., and Petrovich, R. : Synchronous oil migration and cementation in sandstone reservoirs demonstrated by quantitative description of diagenesis [and discussion]: Philosophical Transactions of the Royal Society of London. Series A: Physical and Engineering Sciences, vol. 344, 115-125 (1993)
[39] Gluyas, J. G., Robinson, A. G., Emery, D., Grant, S. M., and Oxtoby, N. H. : The link between petroleum emplacement and sandstone cementation: Petroleum Geology of the North west Europe, Geological Society of London, vol. 4, 1395-1402 (1993)
[40] Bjørnseth, H. M., and Gluyas, J. : Petroleum exploration in the Ula Trend: Norwegian Petroleum Society Special Publications, vol. 4, 85-96 (1995)
[41] Gluyas, J., and Cade, C. A. : Prediction of porosity in compacted sands: In: Reservoir quality prediction in sandstones and carbonates (eds. Kupecz, J. A., Gluyas, J. and Bloch, S.) AAPG Memoir, vol. 69, 19-28 (1997)
[42] Worden, R. H., Oxtoby, N. H., and Smalley, P. C. : Can oil emplacement prevent quartz cementation in sandstones?: Petroleum Geoscience, vol. 4, 129-137 (1998)
[43] Heasley, E. C., Worden, R. H., and Hendry, J. P. : Cement distribution in a carbonate reservoir: recognition of a palaeo oil-water contact and its relationship to reservoir quality in the Humbly Grove field, onshore, UK. Marine and Petroleum Geology, 17, 639-654 (2000). https://doi. org/10.1016/s0264-8172 (99) 00057-4
[44] Marchand, A. M. E., Haszeldine, R. S., Macaulay, C. I., Swennen, R., and Fallick, A. E. : Quartz cementation inhibited by crestal oil charge: Miller deep water sandstone, UK North Sea: Clay Minerals, vol. 35, 201-210 (2000)
[45] Kraishan, G. M., Rezaee, M. R., and Worden, R. H. : Significance of trace element composition of quartz cement as a key to reveal the origin of silica in sandstones: an example from the Cretaceous of the Barrow sub-basin, Western Australia. In: Worden, R. H. & Morad, S. (eds) Quartz Cementation in Sandstones. International Association of Sedimentologists, Special Publications, 29, 317-332 (2000)
[46] Marchand, A. M. E., Haszeldine, R. S., Smalley, P. C., Macaulay, C. I., and Fallick, A. E. : Evidence for reduced quartz-cementation rates in oil-filled sandstones: Geology, vol. 29, 915-918 (2001)
[47] Marchand, A. M. E., Smalley, P. C., Haszeldine, R. S., and Fallick, A. E. : Note on the importance of hydrocarbon fill for reservoir quality prediction in sandstones: American Association of Petroleum Geologists Bulletin, vol. 86, 1561-1571 (2002)
[48] Haszeldine, R. S., Cavanagh, A. J., and England, G. L. : Effects of oil charge on illite dates and stopping quartz cement: calibration of basin models: Journal of Geochemical Exploration, vol. 78-9, 373-376 (2003)
[49] England, G. L., Haszeldine, R. S., Cleverley, J., Barclay, S. A., Yardley, B. W. D., Fisher, Q. J., Graham, C., and Fallick, A. : Applying Ion-Microprobe Technology in Reconstructing Quartz Cement History in an Upper Jurassic Sandstone Reservoir. AAPG Annual Convention, Salt Lake. City, Utah, May 11-14 (2003)
[50] Wilkinson, M., and Haszeldine, R. S. : Oil charge preserves exceptional porosity in deeply buried, overpressured, sandstones: Central North Sea, UK: Journal of the Geological Society, vol. 168, 1285-1295 (2011)
[51] Wilkinson, M., Haszeldine, R. S., and Fallick, A. E. : Hydrocarbon filling and leakage history of a deep geopressured sandstone, Fulmar Formation, United Kingdom: American Association of Petroleum Geologists Bulletin, vol. 90, 1945-1961 (2006)
[52] Higgs, K. E., Zwingmann, H., Reyes, A. G., and Funnell, R. H. : Diagenesis, porosity evolution, and petroleum emplacement in tight gas reservoirs, Taranaki Basin, New Zealand: Journal of Sedimentary Research, vol. 77, 1003-1025 (2007)
[53] Wilkinson, M., Haszeldine, R. S., Ellam, R. M., and Fallick, A. : Hydrocarbon filling history from diagenetic evidence: Brent Group, UK North Sea: Marine and Petroleum Geology, vol. 21, 443-455 (2004)
[54] Ehrenberg, S. N., 1990, Relationship between diagenesis and reservoir quality in sandstones of the Garn Formation, Haltenbanken, mid-Norwegian continental shelf: American Association of Petroleum Geologists Bulletin, v. 74, p. 1538-1558.
[55] Ehrenberg, S. N. : Preservation of anomalously high porosity in deeply buried sandstones by grain-coating

chlorite: examples from the Norwegian continental shelf: American Association of Petroleum Geologists Bulletin, vol. 77, 1260-1260 (1993)
[56] Ramm, M., and Bjorlykke, K. : Porosity depth trends in reservoir sandstones - assessing the quantitative effects of varying pore-pressure, temperature history and mineralogy, Norwegian shelf data: Clay Minerals, vol. 29, 475-490 (1994)
[57] Bjørkum, P. A., and Nadeau, P. H. : Temperature controlled porosity/permeability reduction, fluid migration, and petroleum exploration in sedimentary basins: Australian Petroleum Production and Exploration Association Journal, vol. 38, 453-464 (1998)
[58] Midtbø, R. E. A., Rykkje, J. M., and Ramm, M. : Deep burial diagenesis and reservoir quality along the eastern flank of the Viking Graben. Evidence for illitization and quartz cementation after hydrocarbon emplacement: Clay Minerals, vol. 35, 227-237 (2000)
[59] Aase, N. E., and Walderhaug, A. : The effect of hydrocarbons on quartz cementation: diagenesis in the Upper Jurassic sandstones of the Miller Field, North Sea, revisited: Petroleum Geoscience, vol. 11, 215-223 (2005)
[60] Molenaar, N., Cyziene, J., Sliaupa, S., and Craven, J. : Lack of inhibiting effect of oil emplacement on quartz cementation: Evidence from Cambrian reservoir sandstones, Paleozoic Baltic Basin: Geological Society of Am. Bul., vol. 120, 1280-1295 (2008)
[61] Taylor, T. R., Giles, M. R., et al. : Sandstone diagenesis and reservoir quality prediction: models, myths, and reality. American Association of Petroleum Geologists Bulletin, 94, 1093-1132 (2010). https://doi. org/10.1306/04211009123
[62] Burley, S. D. ; Worden, R. H. : Sandstone. In Sandstone Diagenesis; Recent and, Ancient, Burley, S. D., Worden, R. H., Eds. ; Blackwell Pub. Malden, MA, USA vol. 4, 3-44 (2003)
[63] Sincock, K. J., and Black, C. J. J. : Validation of water/oil displacement scaling criteria using microvisualization techniques. Proceedings of the 64th Annual Technical Conference and Exhibition of the Soc. of Petr. Engineers (San Antonio) S. SPE 18294, 339-347 (1988)
[64] Fassi-Fihri, O., Robin, M., and Rosenberg, E. : Wettability studies at the pore level: a new approach by the use of cryo-scanning electron microscopy. Proceedings of the 66th Annual Technical Conference and Exhibition of the Society of Petroleum Engineers (Dallas), G. SPE 22596, 97-110 (1991)
[65] Worden, R. H., Morad, S. : Quartz cementation in oilfield sandstones: a review of the key controversies. Spec. Publi. Int. Assoc. Sedimentol. 29, 1-20 (2000)
[66] Worden, R. H., and Morad, S. : Clay minerals in sandstones: controls on formation, distribution and evolution. In Worden R. H & Morad S (Eds.), Clay mineral Cements in Sandstones, 34. International Association of Sedimentologists Spec. Pub., 3-41 (2003)
[67] Nguyen, N. T. T., Jones, S. J., Goulty, N. R., Middleton, A. J., Grant, N., Ferguson, A., and Bowen, L. : The role of fluid pressure and diagenetic cements for porosity preservation in Triassic fluvial reservoirs of the Central Graben, North Sea. AAPG Bulletin 97, 1273-1302 (2013)